

AD-A061 700

INCOSYM INC WESTLAKE CA  
INCOFLEX ACCELEROMETER PROGRAM. (U)  
SEP 78 J RUSSELL, R KEMP

F/G 14/2

UNCLASSIFIED

DAAK40-77-C-0181  
NL

1 OF 1  
AD  
A061 700



END  
DATE  
FILMED  
2-79  
DDC

15

DAAK40-77-C-0181

# LEVEL II

12

SC

AD A061700

6

INCOFLEX ACCELEROMETER PROGRAM,

*New*  
INCOSYM, INC.  
780 Lakefield Road  
Westlake, CA 91361

10

J. / Russell  
R. / Kemp

11

Sept ~~1977~~ 1978

12

53 P.

9

FINAL REPORT

Period 19 Aug ~~1977~~ 1977 through 30 Sep ~~1977~~ 1978

DDC FILE COPY

Approved For Public Release, Distribution Unlimited

Prepared For

U.S. ARMY MISSILE R&D COMMAND  
REDSTONE ARSENAL, ALABAMA 35809

DDC  
RECEIVED  
NOV 30 1978  
D

The views and conclusions contained in this document are those of Incosym, Inc., and should not be interpreted as necessarily representing the official policies, either expressed or implied, of the U.S. Army Missile R&D Command or the U.S. Government.

410 953

78 11 13 057

*not*

REPORT DOCUMENTATION PAGE		READ INSTRUCTIONS BEFORE COMPLETING FORM
1. REPORT NUMBER DAAK40-77-C-0181-2/	2. GOVT ACCESSION NO.	3. RECIPIENT'S CATALOG NUMBER
4. TITLE (and Subtitle) INCOFLEX ACCELEROMETER PROGRAM		5. TYPE OF REPORT & PERIOD COVERED FINAL 19 Aug 1977 - 30 Sept 1978
7. AUTHOR(s) J. Russell, R. Knapp		6. PERFORMING ORG. REPORT NUMBER
9. PERFORMING ORGANIZATION NAME AND ADDRESS INCOSYM, INC. 780 Lakefield Road Westlake, CA 91361		8. CONTRACT OR GRANT NUMBER(s) DAAK40-77-C-0181 <sup>la</sup>
11. CONTROLLING OFFICE NAME AND ADDRESS U.S. Army Missile R&D Command Redstone Arsenal, AL 35809		10. PROGRAM ELEMENT, PROJECT, TASK AREA & WORK UNIT NUMBERS
14. MONITORING AGENCY NAME & ADDRESS (if different from Controlling Office)		12. REPORT DATE 30 September 1978
		13. NUMBER OF PAGES 51
		15. SECURITY CLASS. (of this report) Unclassified
16. DISTRIBUTION STATEMENT (of this Report) Approved for public release, distribution unlimited.		15a. DECLASSIFICATION/DOWNGRADING SCHEDULE
17. DISTRIBUTION STATEMENT (of the abstract entered in Block 20, if different from Report)		
18. SUPPLEMENTARY NOTES		
19. KEY WORDS (Continue on reverse side if necessary and identify by block number)		
Accelerometer	Bias	Ternary
Torquing	Scale Factor	Pendulosity
Analog	Suspension	
Digital	Binary	
20. ABSTRACT (Continue on reverse side if necessary and identify by block number)		
<p>The purpose of the contract was to improve the performance of the INCOFLEX<sup>TM</sup> accelerometer; design and develop torquing electronics with a digital output; and build and test one 2 axis and one 3-axis version of the accelerometer. Performance improvement in the long term bias stability and torquer efficiency parameters and determination of the best method of reduction of the scale factor temperature sensitivity were goals of the program. The long term bias stability was improved considerably, and the torquer design optimized as far</p>		

BLOCK 20 Abstract (continued)

→ as possible within the constraints of the design requirements.

Binary, ternary and analog with-conversion-to-digital electronics were built and all three methods operated successfully with the INCOFLEX accelerometer.

A three axis version of the accelerometer was built with analog electronics packaged as part of the unit. A two axis version was built and delivered with separate electronics that can torque the accelerometer in the binary, ternary or analog-with-conversion-to-digital modes.



ACCESSION FOR	
DTIC	White Section <input checked="" type="checkbox"/>
DDI	Buff Section <input type="checkbox"/>
UNANNOUNCED JUSTIFICATION	
BY	
DISTRIBUTION/AVAILABILITY CODES	
Dist.	AVAIL. MOD./OR SPECIAL
A	

DDC  
 RECEIVED  
 NOV 30 1978  
 REGISTRY  
 D

TABLE OF CONTENTS

Section	Title	Page
I	INTRODUCTION . . . . .	I-1
II	LONG TERM BIAS STABILITY . . . . .	II-1
III	TORQUER DESIGN FOR MINIMUM POWER DISSIPATION . . . . .	III-1
IV	TEMPERATURE COEFFICIENT OF THE ACCELEROMETER SCALE FACTOR . . . . .	IV-1
V	TORQUING LOOP ELECTRONICS . . . . .	V-1
VI	DESCRIPTION OF TESTING AND RESULTS . . . . .	VI-1
VII	CONCLUSIONS . . . . .	VII-1
VIII	RECOMMENDATIONS . . . . .	VIII-1

78<sub>i</sub> 11 13 05 7

LIST OF ILLUSTRATIONS

Figure	Title	Page
1	Three Axis Accelerometer . . . . .	I-3
2	Two Axis Incoflex Accelerometer . . . . .	I-4
3	Nondimensional Power Dissipation in Accelerometer Torquer . . . . .	III-2
4	Doped Magnet Peaking At $-2^{\circ}\text{C}$ . . . . .	IV-2
5	Doped Magnet Peaking At $58^{\circ}\text{C}$ . . . . .	IV-3
6	Long Term Bias Stability Accelerometer S/N 8 . . . . .	VI-5
7	Long Term Bias Stability Accelerometer S/N 9 . . . . .	VI-6
8	Short Term Repeatability . . . . .	VI-7
9	Short Term Repeatability . . . . .	VI-8
10	Short Term Repeatability . . . . .	VI-9
11	Short Term Repeatability . . . . .	VI-10
12	Short Term Repeatability . . . . .	VI-11
13	Short Term Repeatability . . . . .	VI-13
14	Short Term Repeatability . . . . .	VI-14
15	Uncompensated Bias Temperature Sensitivity - S/N 7S . . . . .	VI-15
16	Uncompensated Bias Temperature Sensitivity - S/N 8 . . . . .	VI-16
17	Uncompensated Bias Temperature Sensitivity - S/N 9 . . . . .	VI-17
18	Uncompensated Bias Temperature Sensitivity - S/N 10 . . . . .	VI-18
19	Bias Drift Accelerometer S/N 8 . . . . .	VI-19
20	Bias Drift Accelerometer S/N 9 . . . . .	VI-20
21	Bias Drift Accelerometer S/N 10 . . . . .	VI-21
22	Bias Temperature Sensitivity - S/N 8 in VRM . . . . .	VI-22
23	VRM Short Term Bias Repeatability . . . . .	VI-23
24	VRM Scale Factor Temperature Sensitivity . . . . .	VI-26
25	Bias Vs Pickoff Excitation Frequency . . . . .	VI-27
26	Analog Conversion-Ternary Output Vs Temperature . . . . .	VI-29
27	Short Term Repeatability S/N 10 . . . . .	VI-30
28	Short Term Repeatability with Digital Output S/N 10 . . . . .	VI-31

LIST OF TABLES

Table	Title	Page
I	COMPARISON OF TORQUING ELECTRONICS . . . . .	V-2
II	SUMMARY OF ACCELEROMETER PERFORMANCE . . . . .	VI-3
III	ACCELEROMETER NO. 9 PARAMETERS VERSUS TEMPERATURE CYCLES . . . . .	VI-4
IV	SUMMARY OF VRM PERFORMANCE . . . . .	VI-24
V	VRM TORQUER SCALE FACTOR . . . . .	VI-25
VI	VRM INPUT RANGE . . . . .	VI-25
VII	VRM CAGING LOOP BANDPASS . . . . .	VI-25
VIII	POWER SUPPLY VOLTAGE SENSITIVITY . . . . .	VI-28

## I. INTRODUCTION

Presented is the final technical report covering the accelerometer program sponsored by the U.S. Army Missile R&D Command under contract number DAAK40-77-C-0181.

The objective of the program was to improve the performance of the INCOFLEX<sup>TM</sup> accelerometer; design and develop torquing electronics with a digital output; and build and test one 2-axis and one 3-axis version of the accelerometer.

Performance improvement considerations in the program were to improve the long term bias stability (the goal was less than 40  $\mu$ gs one sigma), determine the best way to decrease the scale factor temperature sensitivity and improve the torquer efficiency, i.e., reduce the power requirement for any given pendulosity.

To improve the long-term bias stability, the suspension and case were modified which also resulted in less parts. The suspension and case now are combined and manufactured as one part. The test results indicated the repeatability, after exposure to temperatures between  $-65^{\circ}\text{F}$  and  $210^{\circ}\text{F}$ , was improved from the previous units built.

An analysis was conducted to determine the best method of reducing the scale factor temperature coefficient. Use of "doped" magnet material, compensating magnet material or electrical compensation were examined. Electrical compensation was determined to be the best approach, and the design of the accelerometer was modified to incorporate a suitable electrical compensation sensor.

The torquer design was analyzed and modification made to the extent possible. Limitations in the available space and constraints on the practicality of small airgaps only yielded a slight improvement in the torquer efficiency.

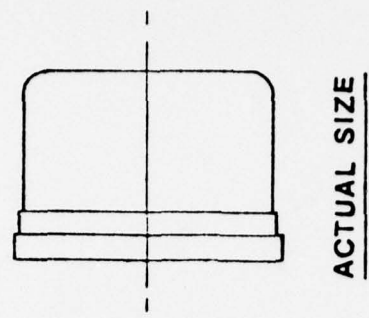
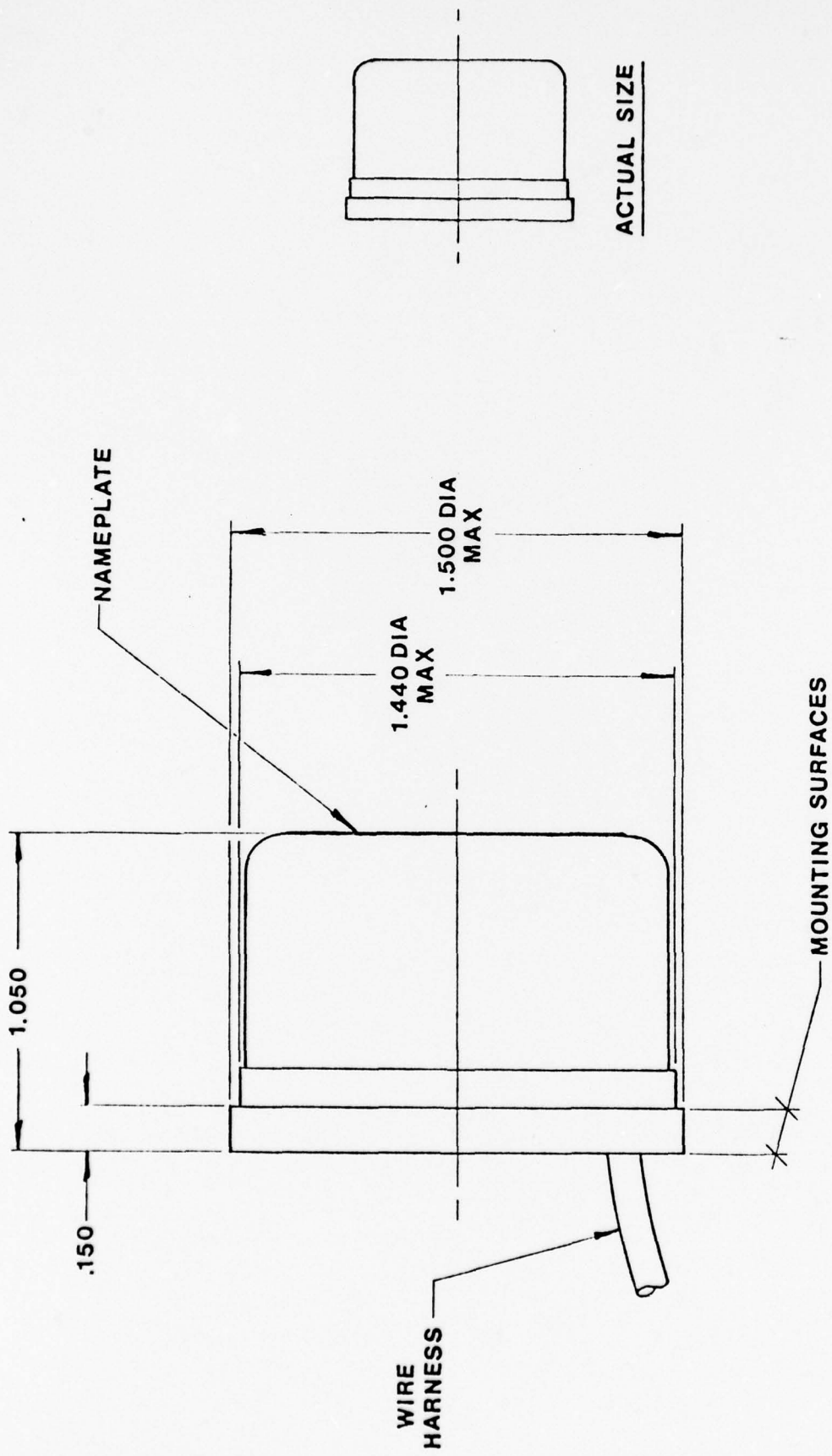
Three possibilities were considered for the torquing electronics with a digital output. These were binary pulse torquing, ternary pulse torquing and analog with analog-to-digital conversion. It was concluded that as the application may be influential in prescribing the specific method, and as various applications are possible, all three methods would be developed and tested. This was done utilizing the maximum number of common components between each

method. Breadboard electronics of all three methods were built and tested with the two-axis accelerometer and delivered to U.S. Army Missile R&D Command.

The three-axis accelerometer was built and integral analog electronics were packaged with it. Because of a system interface already established for a potential application, the accelerometer internal temperature sensor could not be utilized for correction of temperature coefficients. However, the temperature sensor required by the application was added to the outside of the package. The only drawback to this is the temperature sensor is not in the correct location to correct for transient temperature changes.

Figure 1 shows the outline and mounting drawing for the three-axis package, including the electronics. The electronics are all discrete commercially available components. Figure 2 shows the outline and mounting drawing for the two-axis accelerometer, which does not contain integral electronics for this program.





TWO AXIS INCOFLEX  
ACCELEROMETER

Figure 2.

## II. LONG TERM BIAS STABILITY

Examination of the design indicated that a possible improvement of the long term bias stability could be accomplished if there were less connecting mechanical joints between the case, suspension and pendulous mass. Therefore, the design was modified so that the case and suspension could be made from one piece. This had the added advantage of eliminating parts, therefore reducing the potential cost. The design was modified and the accelerometers for the program were fabricated utilizing this approach. As the length of the program did not allow for bias stability readings to be accrued over a long period of time, it was decided to cycle the accelerometers many times over temperature extremes of  $-65^{\circ}\text{F}$  to  $+210^{\circ}\text{F}$  and record the bias. The temperature range used is larger than the worst case operational conditions but was used to induce bias changes. Under these conditions, the one sigma values of the four axes tested were 93, 56, 70 and 40  $\mu\text{g}'\text{s}$ .

### III. TORQUER DESIGN FOR MINIMUM POWER DISSIPATION

Within the confines of the existing design concept, the power dissipation at a given level is a function of magnetic material used, torquer geometry and the level of leakage fluxes. The magnetic material used in the existing design is Samarium Cobalt, which is considered an optimum choice at this time due to long-term stability and high energy product. Torquer geometry, particularly that involving the ratio of the length of the airgap to the length of the magnet, was investigated in detail. It was concluded that there was an optimum ratio at which the power consumption is a minimum. Figure 3 shows curves relating the non-dimensional power dissipation parameter,  $P$ , with the ratio  $R$  equal to airgap length. It is observed from this curve that the minimum power dissipation is not only a function of the ratio  $R$  but also is dependent on the leakage factor.

The ratio of airgap length to magnet length on the design is 125. This is the same as for the original design. Because of the fabrication difficulty if the airgap length is reduced, and as the desired size of the completed unit precluded any increase in magnet length, it was decided not to change either of these parameters. The leakage flux was also as low as seemed practical on the initial design. However, it was concluded that an increase in the number of turns on the torquer coil may be possible. Experimentation resulted in an increase of 10 percent in this area without changing wire size.

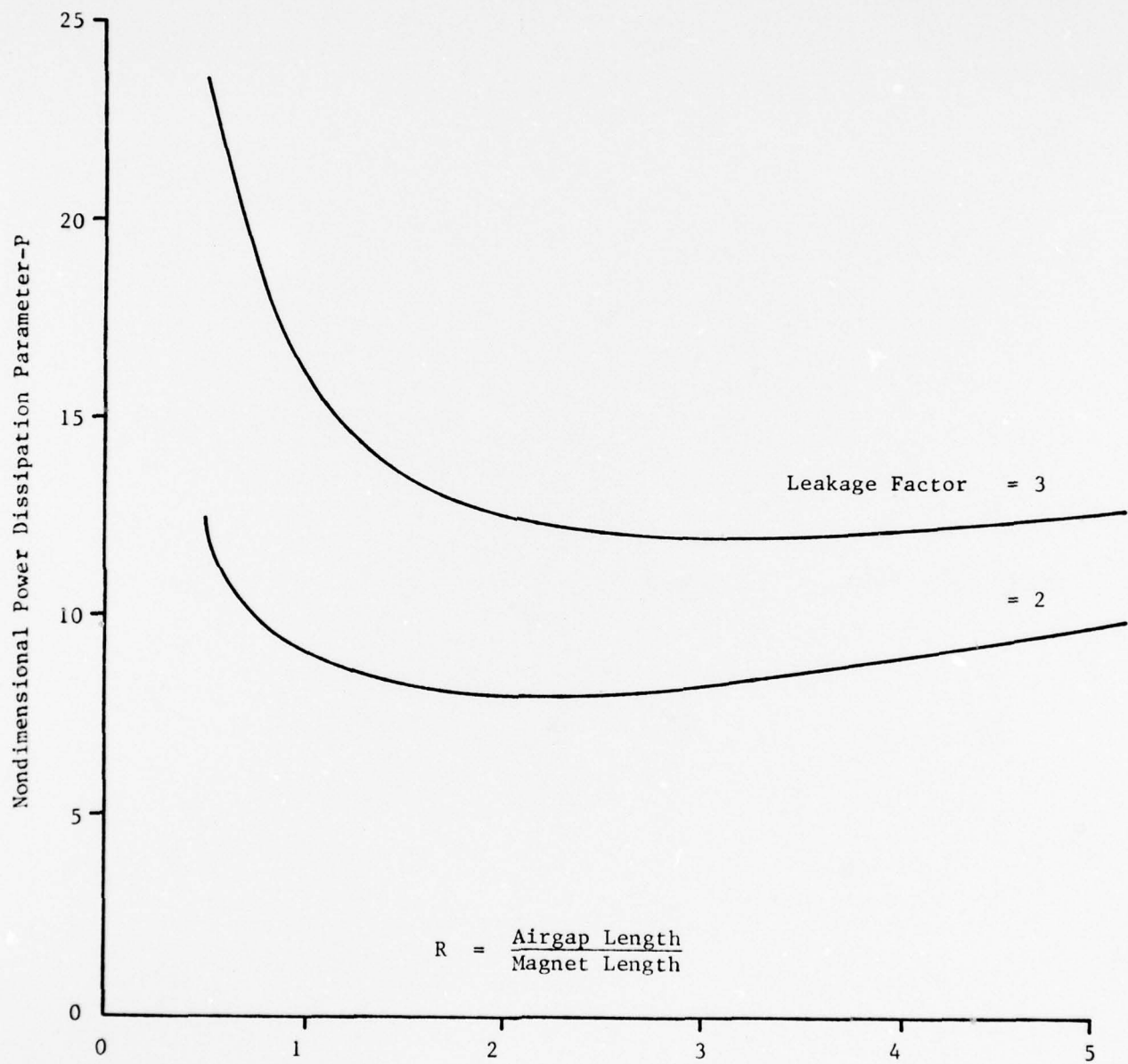


Figure 3. Nondimensional Power Dissipation in Accelerometer Torquer

#### IV. TEMPERATURE COEFFICIENT OF THE ACCELEROMETER SCALE FACTOR

In the present design, the temperature coefficient of the scale factor is fully accounted for by the temperature coefficient of the Samarium Cobalt magnet. Data provided by the magnet manufacturer indicates a negative coefficient in the range of 400 PPM/°C to 450 PPM/°C and the data measured was -425 PPM/°C. Three methods of reducing scale factor temperature coefficient were investigated. These methods were:

- (1) Use of "doped" Samarium Cobalt material
- (2) Use of compensating magnet material
- (3) Use of compensation methods based on sensor temperatures

The doped Samarium Cobalt magnet has a reversible temperature coefficient an order of magnitude smaller than the "undoped" material. Figures 4 and 5 show magnetization curves for two doped experimental magnets. It is noted the curves are nonlinear and the "peaking" temperature can be changed by composition and process control. It is also noted that doping reduces the energy product from 20 MGO<sub>e</sub> to about 12 MGO<sub>e</sub>. The reduction of the energy product is the major disadvantage to this approach, and would negate the efforts to improve the torquer efficiency. Also, concern over the long term stability of the magnetic properties after it has been "doped" make this approach precarious.

The temperature coefficient of the magnet can also be controlled by the use of compensating material in which the permeability changes with temperature. Due to the non-linear characteristics of the compensating material, linear compensation cannot be obtained over a broad temperature range. Another area of concern when using this method of compensation is the magnetic instability of the compensating material itself after exposure to temperatures encountered in actual applications. Any instability of the compensating material will cause an accelerometer scale factor change.

Compensation based on sensed temperature seems to be the most promising because of linearity and predictability of the temperature coefficient of Samarium Cobalt material over a wide temperature range. Also, all accelerometers have exactly the same scale factor temperature coefficient, allowing

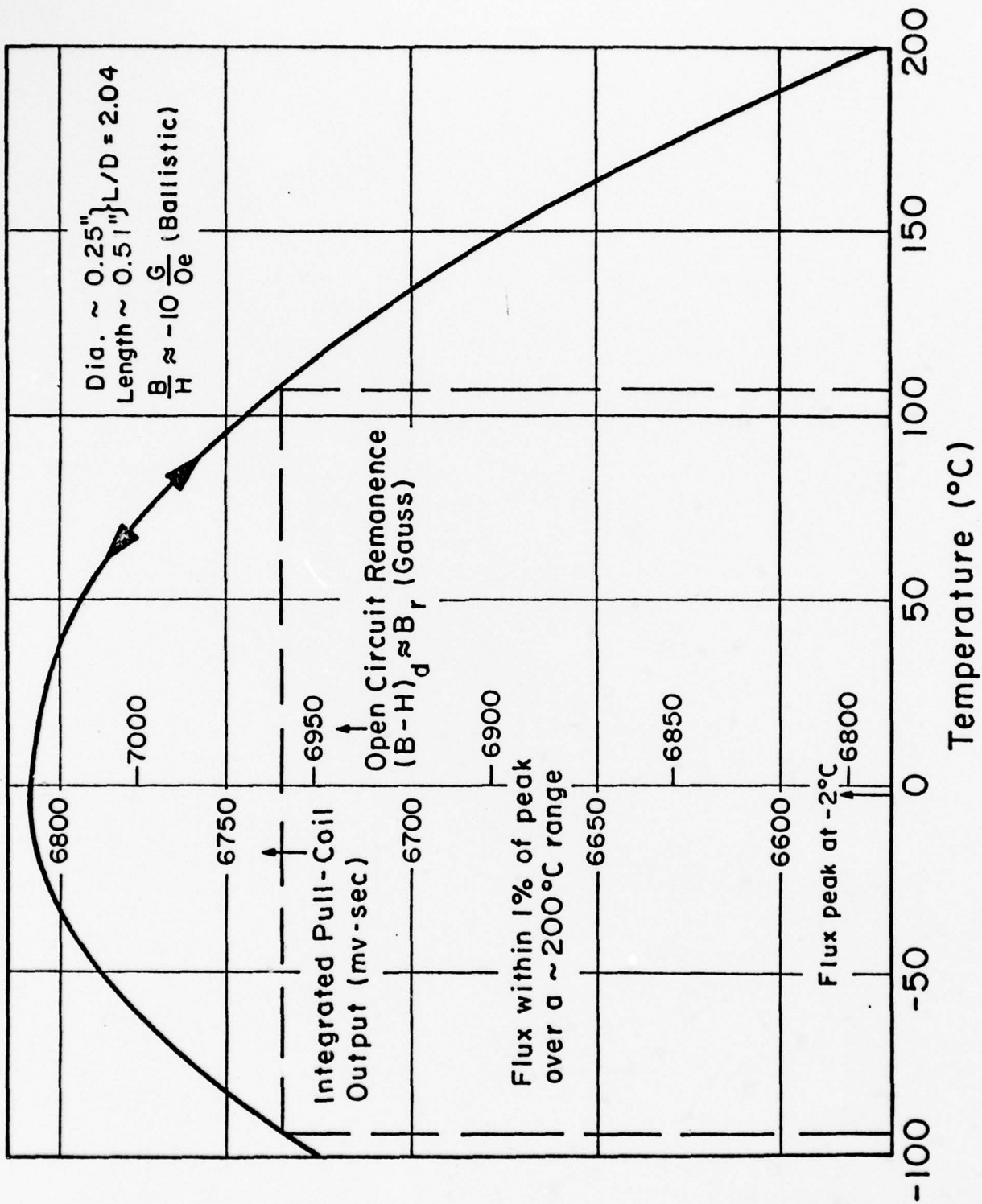


Figure 4. Doped Magnet Peaking At  $-2^\circ\text{C}$

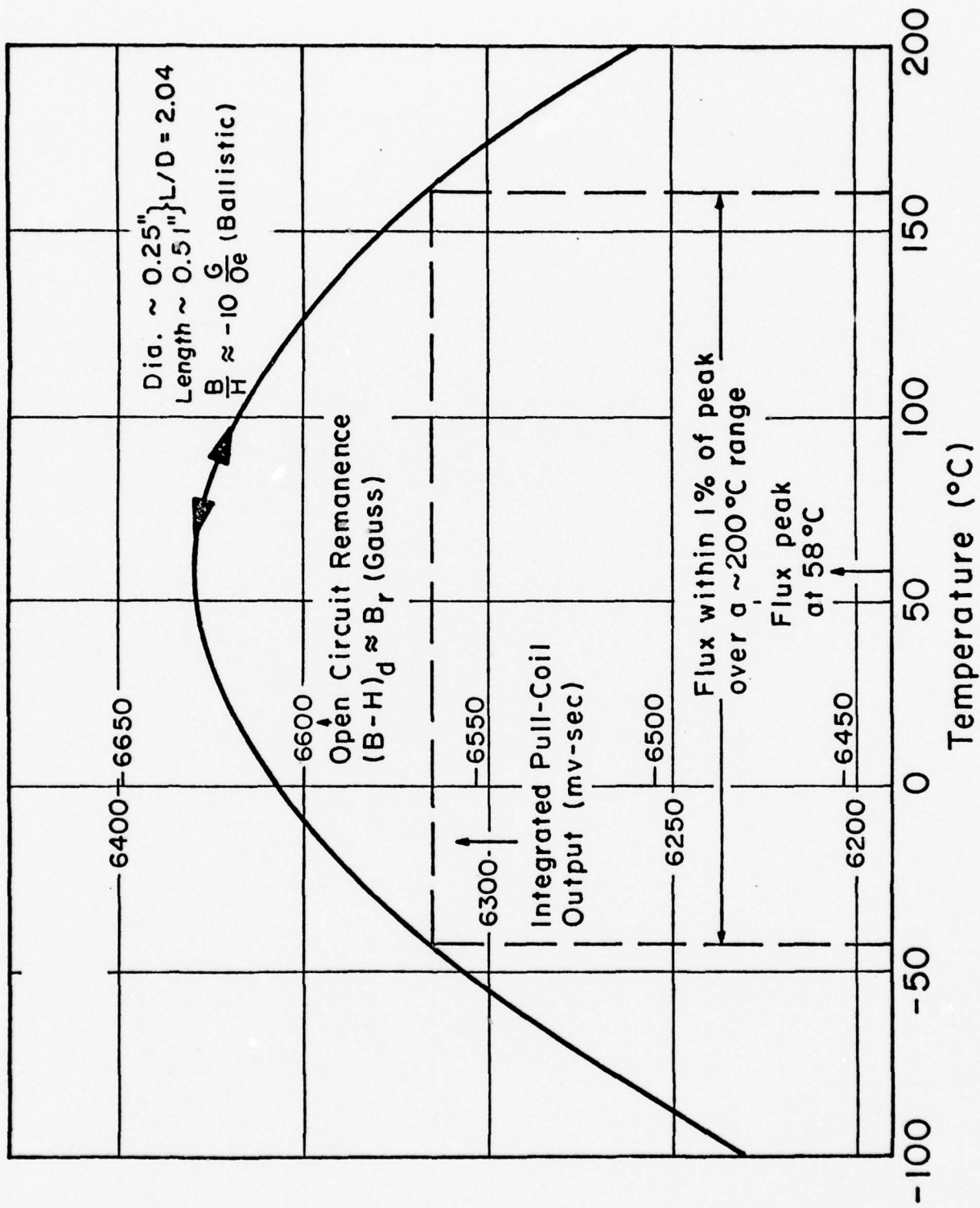


Figure 5. Doped Magnet Peaking At  $58^\circ C$

Interchangeability. The accuracy of compensation depends mainly upon the ability to measure accurately the temperature of the magnets. It is not convenient to perform this measurement directly as contact with the magnet material is difficult. In view of this, the placement of the temperature sensor is of importance, particularly during transient conditions. Therefore, a design modification was made to locate the temperature sensor in an optimum location. Also, the type of sensor is important so that good resolution can be obtained with good stability over a long period of time. It was decided to incorporate an AD 590 in the design. Although rather large in size when compared to the accelerometer, it was possible to allocate enough space and the sensor was incorporated in the build of the deliverable units. The AD 590 has a scale factor of  $1 \mu\text{a}/^{\circ}\text{C}$  that is linear to better than 1 percent from  $-55^{\circ}\text{C}$  to  $+125^{\circ}\text{C}$ .

## V. TORQUING LOOP ELECTRONICS

Three possibilities were considered for the torquing loop. These were:

- (1) Use of binary torquing
- (2) Use of ternary torquing
- (3) Use of analog with an analog-to-digital conversion

All three approaches produce a digital output. The binary approach torques the accelerometer with a square wave at constant power. The power must be sufficient to torque the accelerometer at the maximum acceleration, typically 10 to 15 g's. This means the maximum power is constantly dissipated in the accelerometer and electronics. The ternary approach also torques the accelerometer with a square wave, but the power is on demand, i.e., maximum power is only required at maximum acceleration, and zero power is required when no acceleration is present. The analog with conversion approach torques the accelerometer with a DC voltage which supplied power on demand.

After consideration of the options, it was decided to build electronics for all three approaches and compare the results. All three methods were designed and built and operated successfully with the INCOFLEX<sup>TM</sup> accelerometer. A comparison of the three methods is shown in Table I.

The most significant factor is that the bias stability and bias temperature coefficient is significantly higher in the binary approach. This is because the torquing current through the electronics in the steady state condition is ten (10) times higher than for the other two approaches. Therefore, any bias change in the electronics is magnified. The higher torquing current also heats the electronics more, so the settling (reaction) time is longer.

The only major difference between the ternary and analog approaches is in the bandwidth capability. It is easier to get a higher bandwidth with the analog approach than with either the ternary or binary. The respective bandwidths that have been set for the present electronics is shown in Table I. Although this can be adjusted, and it would be possible to increase the ternary and binary bandwidths, the analog bandwidth will always be inherently higher than the other two. The only factor that is not superior in the analog approach

TABLE I. COMPARISON OF TORQUING ELECTRONICS  
 Electronics only. Does not include accelerometer parameters.

	Analog with Conversion	Ternary	Binary
Scale Factor Stability	Same ( $\approx 10$ ppm)	Same ( $\approx 10$ ppm)	Same ( $\approx 10$ ppm)
Bias Stability	Same ( $\approx 1$ $\mu\text{g}$ )	Same ( $\approx 1$ $\mu\text{g}$ )	Approx. 10X higher ( $\approx 10$ $\mu\text{g}$ )
Scale Factor Temperature Coefficient	Same ( $\approx 15$ ppm/ $^{\circ}\text{F}$ )	Same ( $\approx 15$ ppm/ $^{\circ}\text{F}$ )	Same ( $\approx 15$ ppm/ $^{\circ}\text{F}$ )
Bias Temperature Coefficient	Same ( $\approx 1$ $\mu\text{g}/^{\circ}\text{F}$ )	Same ( $\approx 1$ $\mu\text{g}/^{\circ}\text{F}$ )	Approx. 100X worse ( $\approx 10$ $\mu\text{g}/^{\circ}\text{F}$ )
Linearity	Same	Same	Same
Bandwidth	Highest (Min. 250 Hz)	Lower (Approx. 100 Hz)	Lower (Approx. 100 Hz)
Reaction Time	Short (10 sec. max.)	Short (10 sec. max.)	Longer (30 sec. min.)
Power	Minimum	Minimum	Maximum
Component Count	Slightly Higher (5%) than ternary	Nominal	Slightly Lower (5%) than ternary

is that the parts count is slightly higher. However, the slight increase (approximately 5 percent over ternary and 10 percent over binary) is justified relative to the advantages.

The electronics for the three axis accelerometer are packaged as part of the unit, and provide only an analog output as required by specification. The electronics for the two axis accelerometer are on separate boards and have the capability of providing any three of the torquing methods.

## VI. DESCRIPTION OF TESTING AND RESULTS

As the output of the accelerometer is a DC voltage scaled for one (1) volt per g, the readout for testing was a precision differential voltmeter driving a chart recorder. Because this is a two axis accelerometer, two channels were needed. Consequently, two identical Hewlett Packard 3420 Differential Voltmeters, each driving one axis of a two axes Hewlett Packard 7130 A chart recorder, were utilized.

The accelerometer was mounted on a base plate that was fastened into a granite cube. The cube was placed on a granite table. As the faces of the cube are flat and orthogonal to each other, the accelerometer could be tested by rotating the cube on to each of its faces, therefore precisely changing the gravity vector applied to the accelerometer. The base plate had heaters installed so that temperature effects on the accelerometer could be measured by changing the temperature.

All or part of the following tests were performed on accelerometers S/N 7S (single axis), 8, 9 and 10.

- (1) Parameter stability tracking over several days, with remounting and extensive temperature cycling. Parameters are bias, scale factor, torquer axis alignment and pendulosity.
- (2) Bias repeatability over short periods of time with pendulous axis both vertical and horizontal.
- (3) Uncompensated bias temperature sensitivity.
- (4) Drift tests (two and twelve hours).
- (5) Pendulous axis alignment.
- (6) Reaction time.

Accelerometers S/N 7S and 8 were then installed in the Velocity Reference Module (VRM) with self contained analog electronics, and tested as follows:

- (1) Bias temperature sensitivity, X and Y axes.
- (2) Turn on bias repeatability over short periods of time with X, Y and Z at 0 "g".

- (3) Scale factor determination X, Y and Z axes.
- (4) Scale factor temperature coefficient Z axis.
- (5) Caging loop bandwidth X, Y and Z axes.
- (6) Input range (calculated).
- (7) Pickoff excitation frequency sensitivity.
- (8) Power supply voltage sensitivity.

Accelerometers 9 and 10 were used during the evaluation of the digital electronic circuits. Limited digital data was obtained using No. 9 because the instrument was damaged during handling. Accelerometer No. 10 was therefore used for most of the digital electronic testing. Five modes of operation are possible with the delivered electronics; analog cage with analog readout, analog cage with digital binary readout, analog cage with digital ternary readout, digital cage with binary readout and digital cage with ternary readout. Performance data presented is the mode of analog cage with ternary readout. Subtests of the digital conversion circuits are also presented.

The summary of test results are shown in Table II.

Table III and Figures 6 and 7 are included in the following to show the stabilizing influence of temperature soaking and extensive temperature cycling on accelerometers No. 8 and 9. After the stabilizing shown the X and Y bias repeatability on No. 8 were 93  $\mu\text{g}$  and 70  $\mu\text{g}$ . On No. 9 it was 56  $\mu\text{g}$  and 40  $\mu\text{g}$ . This long term bias stabilizing process is done on all accelerometers.

Accelerometers No. 7S, 8 and 9 were tested for short term turn on repeatability and results are shown in Figures 8 through 12. The average of all pendulous axis vertical tests was 14.7  $\mu\text{g}$  (1 $\sigma$ ). The average of all pendulous axis horizontal tests was 23.2  $\mu\text{g}$  (1 $\sigma$ ).

It was subsequently discovered that the electronic caging loop caused some degradation in the short term repeatability performance. When turning on the instrument, a torquer current transient caused the pendulous element to forcefully hit the stop before a stable caged condition could be established. Once discovered, a different turn on method was used when accelerometer No. 10 was evaluated. Although the short term repeatability of No. 7S, 8 and 9 was

TABLE II. SUMMARY OF ACCELEROMETER PERFORMANCE

Parameter	Units	Goal	Measured (X Axis/Y Axis)			
			#7S	#8	#9	#10
Short term repeatability PAV	$\mu\text{g}$ (1 $\sigma$ )	10	3.3	13/17	28/22	3.3/2.9
Short term repeatability PAH	$\mu\text{g}$ (1 $\sigma$ )	10	8.4	14/26	18/40	2.9/2.5
Long term bias stability (4)	$\mu\text{g}$ (1 $\sigma$ )	40 <sup>(5)</sup>	N.M.	93/70	56/40	N.M.
Bias temperature sensitivity <sup>(1)</sup>	$\mu\text{g}/^\circ\text{F}$ (2)	1	-6.7	-8/-5	+1/-5	-1.2/+2.8
Bias drift (two hour)	$\mu\text{g}$ (1 $\sigma$ )	2	-	1.0/1.8 <sup>(3)</sup>	1.8/2.7 <sup>(3)</sup>	.5/1.4
Axis alignment	arcsecond	62	37	9.2	14.8	17.3
Reaction time	second	3	3	3	3	3

(1) Uncompensated

(2) 100°F temperature change

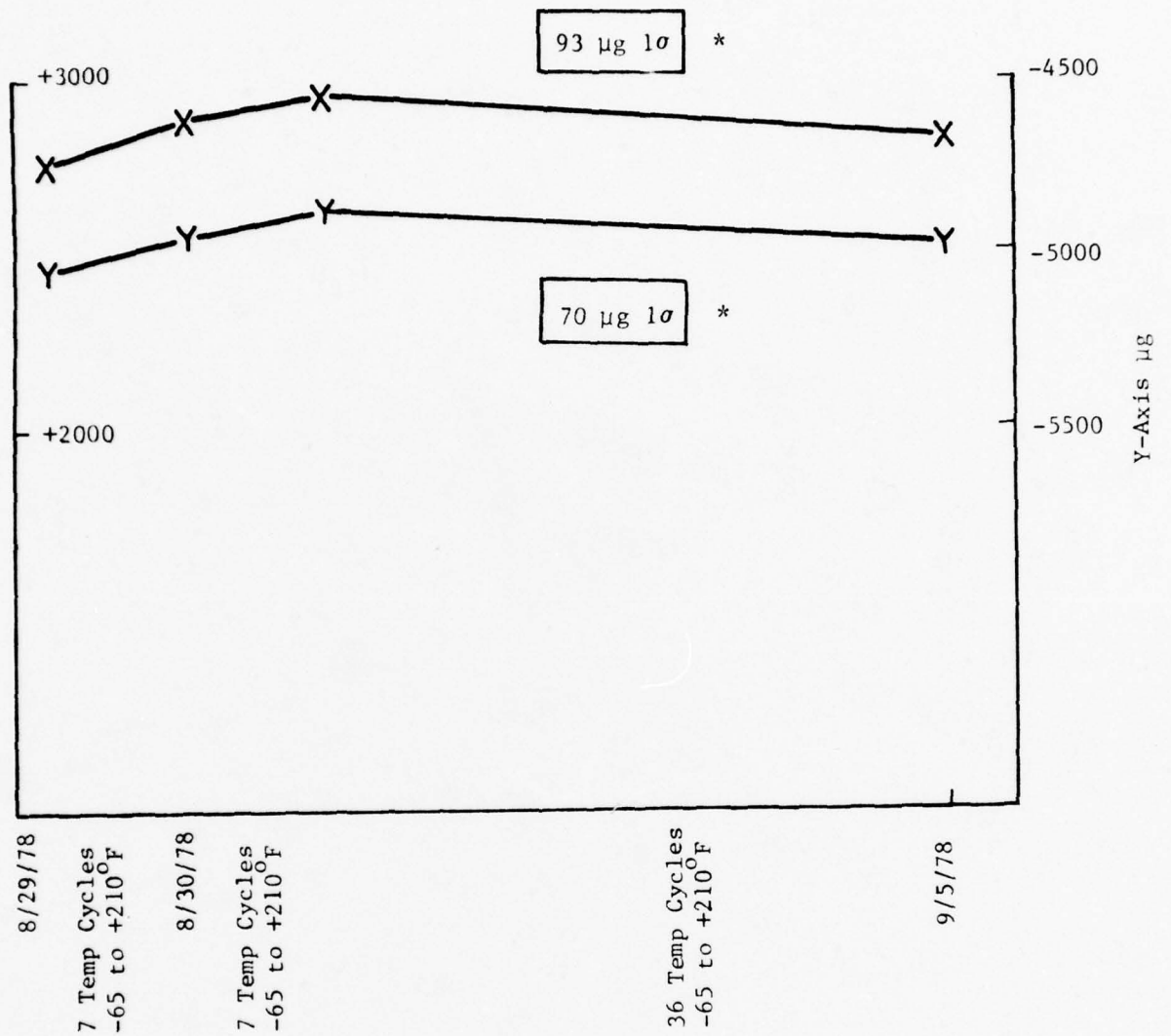
(3) X and Y data taken over 12 hours

(4) Including temperature cycling -65°F to +210°F and remounting

(5) Does not include exposure to -65 to +210°F

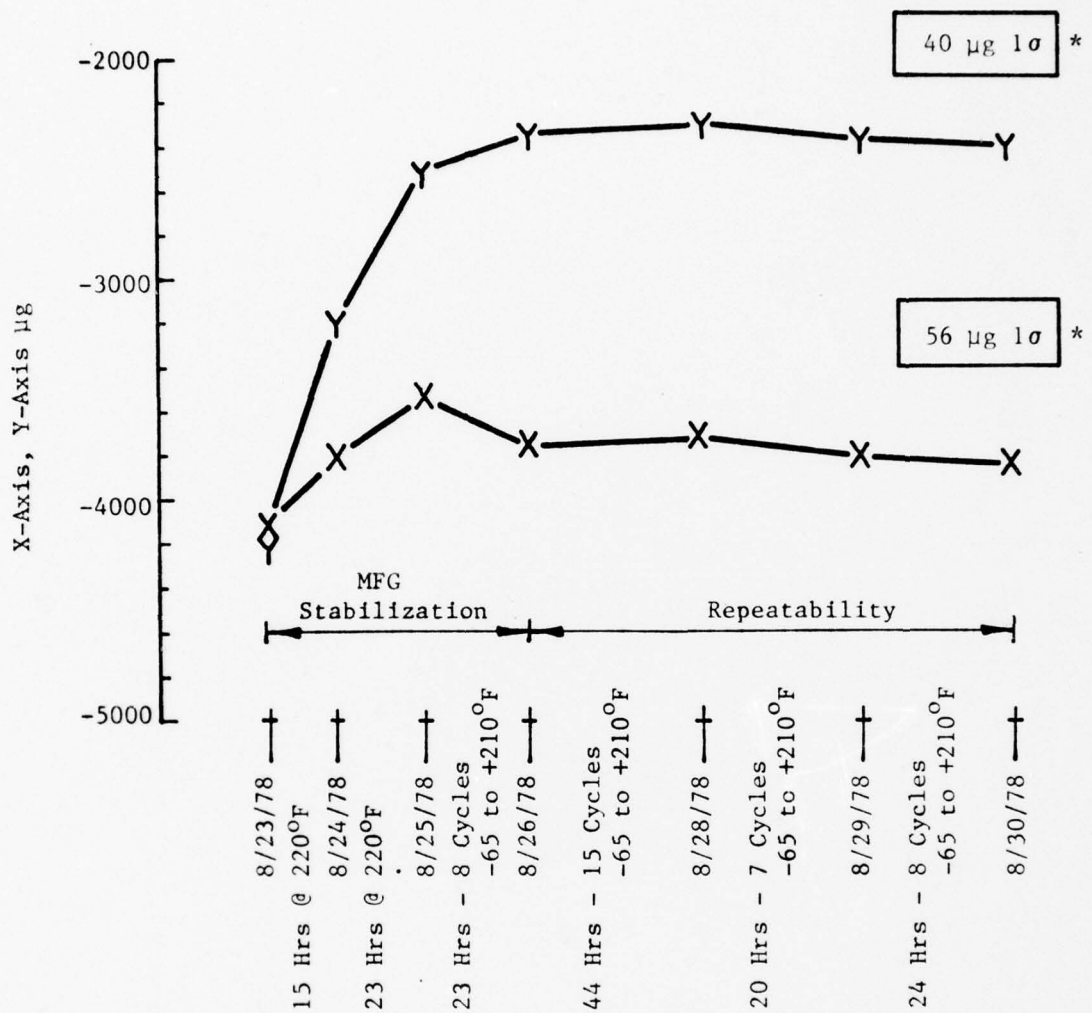
TABLE III. ACCELEROMETER NO. 9 PARAMETERS VERSUS TEMPERATURE CYCLES

	8/23/78	8/24/78	8/25/78	8/26/78	8/28/78	8/29/78	8/30/78
$B_{XH} - \mu g$	-4054	-3803	-3575	-3749	-3685	-3795	-3808
$B_{YH} - \mu g$	-4177	-3018	-2553	-2387	-2291	-2327	-2344
$B_{XV} - \mu g$	-4047	-3850	-3575	-3759	-3672	-3832	-3808
$B_{YV} - \mu g$	-4216	-3040	-2561	-2385	-2370	-2385	-2401
$K_X g/v$	1.3017	1.3013	1.3013	1.3014	1.3016	1.3015	1.3015
$K_Y g/v$	1.3214	1.3211	1.3209	1.3212	1.3213	1.3212	1.3208
$\alpha$ mrad	+5.47	+5.52	+6.16	+5.19	+5.60	+5.49	+4.97
$\beta$ mrad	+4.86	+4.91	+5.55	+4.55	+4.93	+4.85	+4.36
$\gamma_X$ mrad	-14.34	-14.24	-14.35	-14.29	-14.34	-14.26	-14.37
$\gamma_Y$ mrad	+28.10	+28.02	+28.04	+28.02	+28.07	+28.09	+28.0
		15 Hours At 220°F	23 Hours At +220°F	23 Hours - 8 Cycles -65 to +220°F	44 Hours - 15 Cycles -65 to +210°F	20 Hours - 7 Cycles -65 to +210°F	24 Hours - 8 Cycles -65 to +210°F



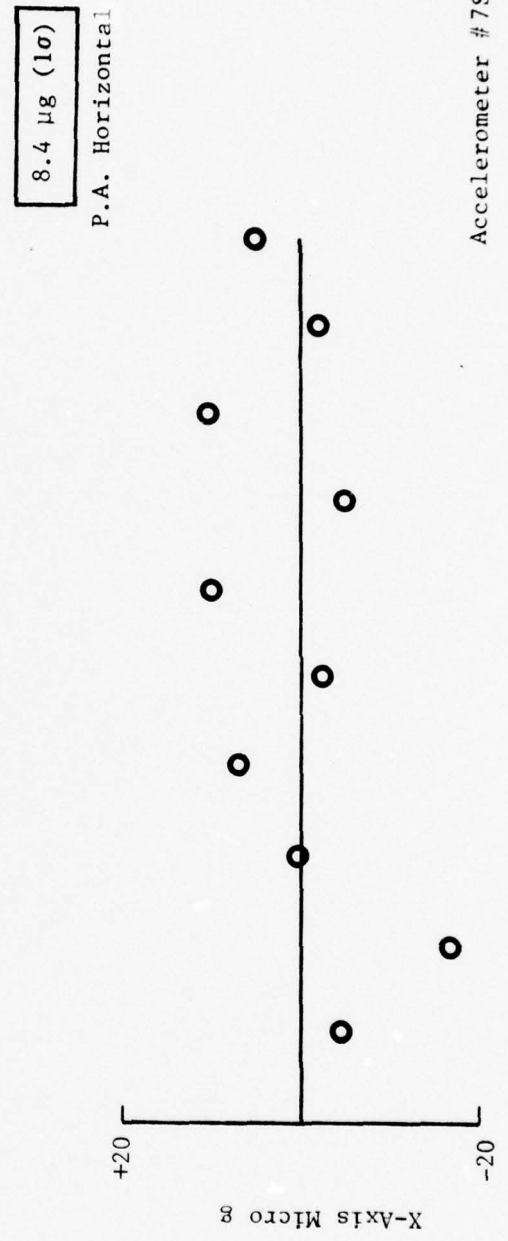
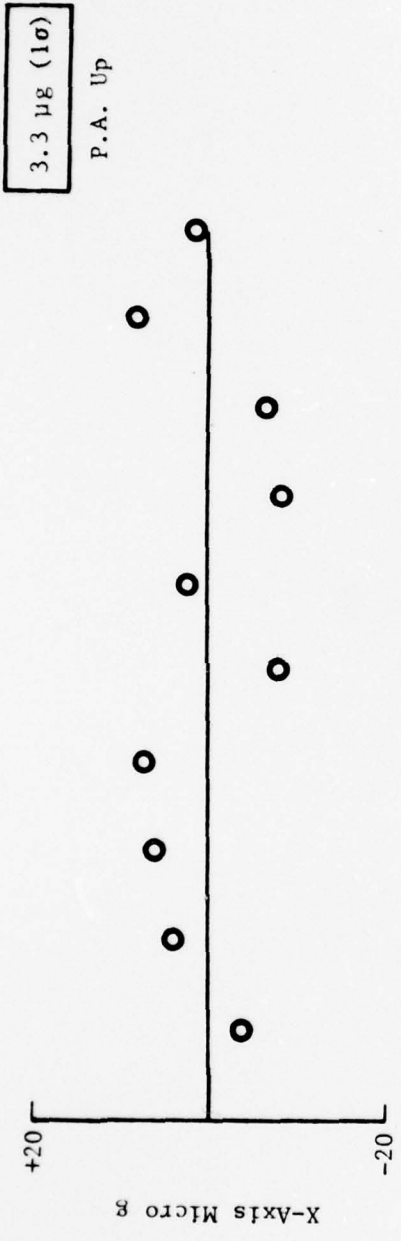
\*Includes remounting, temperature cycling and shutdown repeatability

Figure 6. Long Term Bias Stability Accelerometer S/N 8



\*Includes remounting and temperature cycling and shutdown repeatability.

Figure 7. Long Term Bias Stability Accelerometer S/N 9



Accelerometer #7S

Figure 8. Short Term Repeatability

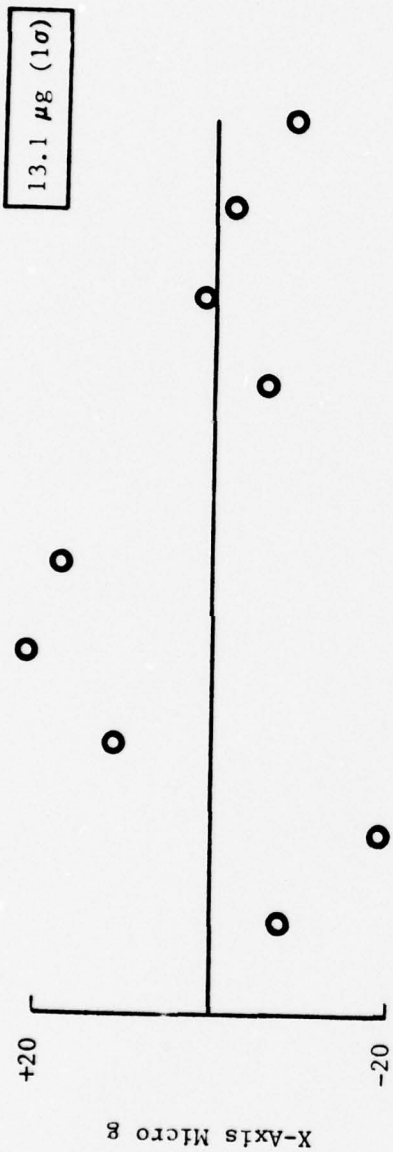
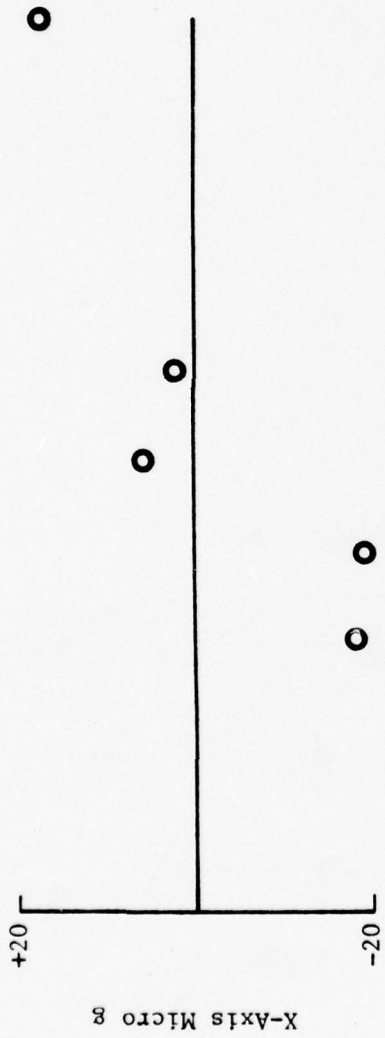
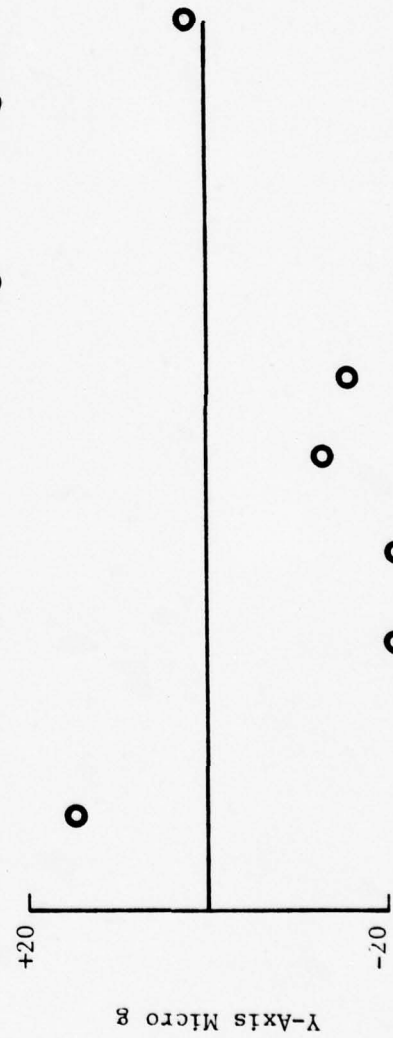


Figure 9. Short Term Repeatability

27.5  $\mu\text{g}$  ( $1\sigma$ )



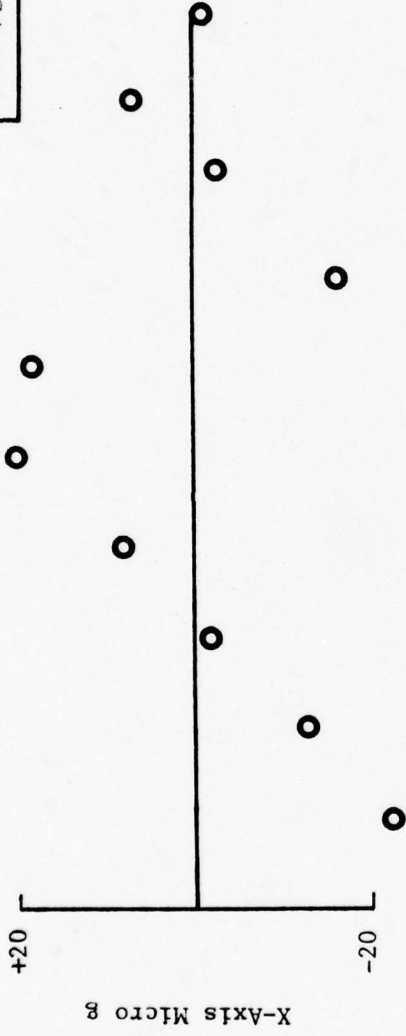
22.3  $\mu\text{g}$  ( $1\sigma$ )



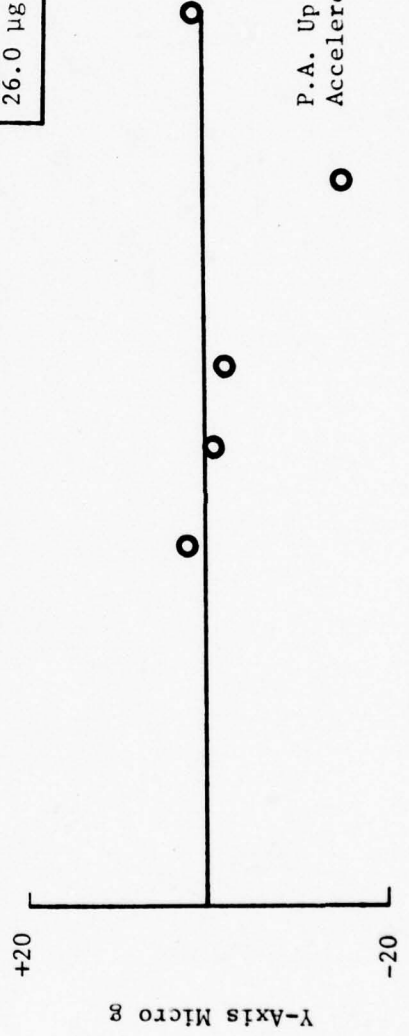
P.A. Horizontal  
XT Down  
Accelerometer #8

Figure 10. Short Term Repeatability

14.0  $\mu\text{g}$  ( $1\sigma$ )



26.0  $\mu\text{g}$  ( $1\sigma$ )



P.A. Up  
Accelerometer #9

Figure 11. Short Term Repeatability

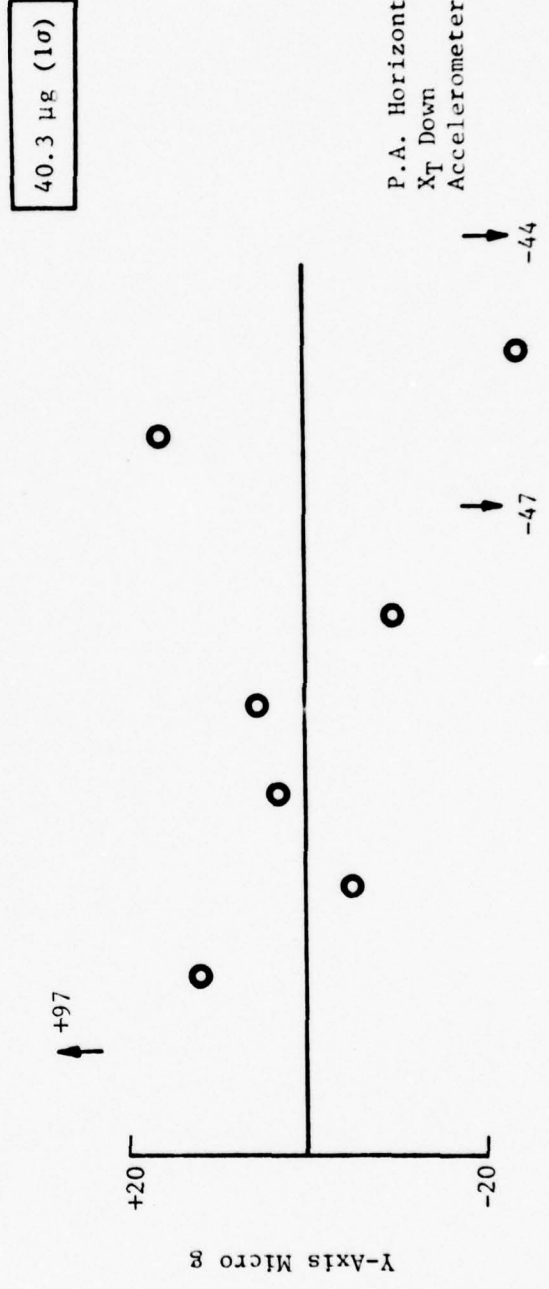
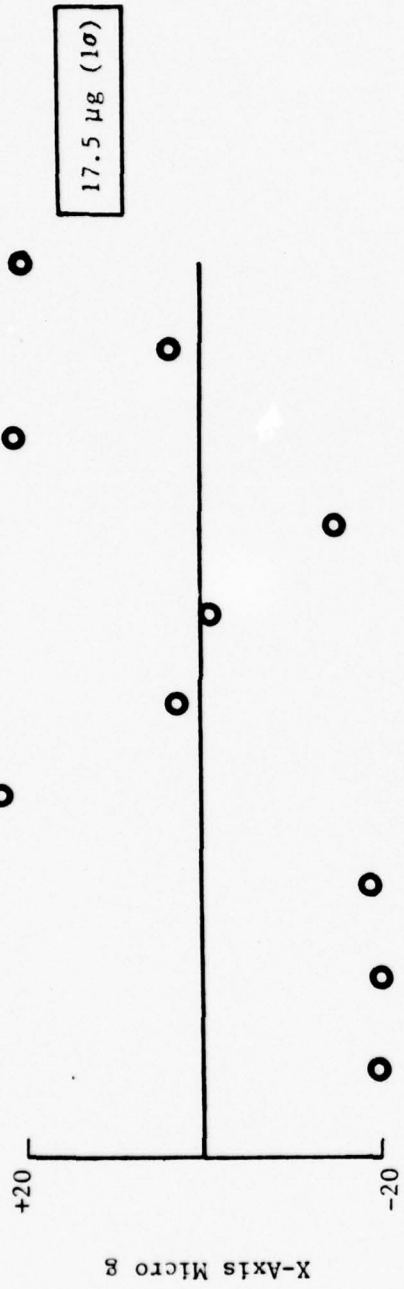


Figure 12. Short Term Repeatability

quite good, No. 10 was significantly better as shown in Figures 13 and 14. The pendulous axis horizontal test result was  $2.9 \mu\text{g}$  and  $2.5 \mu\text{g}$  ( $1\sigma$ ). The pendulous axis vertical test result was  $1.2 \mu\text{g}$  and  $1.4 \mu\text{g}$  ( $1\sigma$ ). A change was made in the electronic box to avoid the problem in future testing.

Figures 15, 16, 17 and 18 show the bias temperature coefficients without compensation. In all cases this parameter was linear, allowing for simple modelling and easy compensation if required. Five of the seven axes evaluated had exceptionally low values.

A long term bias drift test was performed on accelerometers 8 and 9. Bias was monitored for 12 hours in the pendulous axis vertical position. The average drift of the four axes measured was  $1.8 \mu\text{g}$  ( $1\sigma$ ) over 12 hours. A two hour drift test was also performed on accelerometer No. 10 with both axes less than  $1.5 \mu\text{g}$  ( $1\sigma$ ). See Figures 19, 20 and 21.

The axes alignment to the case was adjusted and measured to be  $.18$  mradian on the single axis accelerometer and less than  $.06$  mradian on the remaining two accelerometers. This parameter is easily adjusted and is well within the design specification of  $.3$  milliradian.

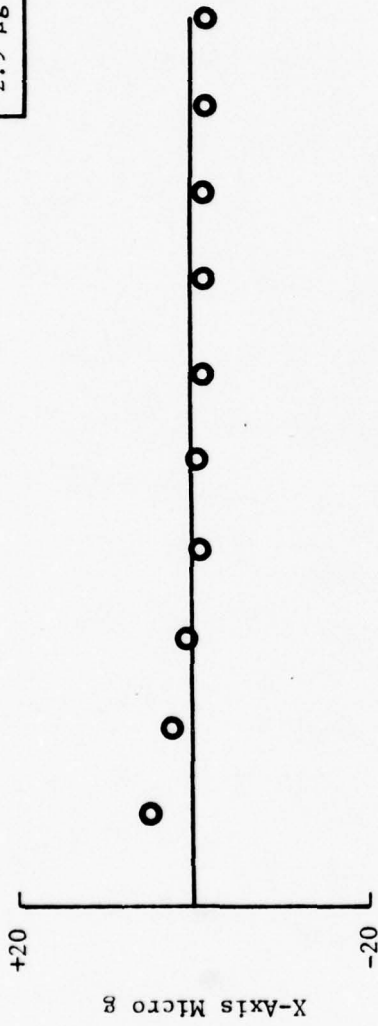
The reaction time of all axes tested was measured to be less than 3 seconds. This includes the test stand electronic caging loop.

When S/N 7S and 8 were installed in the VRM the bias temperature stability was remeasured on the VRM X and Y axes. The results are shown on Figure 22 and agree with the test results of accelerometer No. 8.

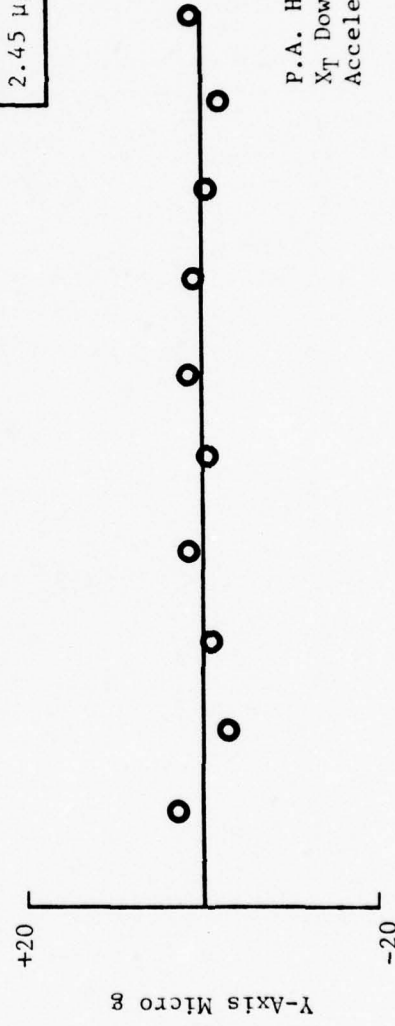
Short term turn on repeatability was tested on the VRM by turning the common power supply off and on. The slower change in power supply voltage avoided the current transient previously described. Better results were obtained when testing accelerometer No. 7S and 8 in the VRM than in the test station, (see Figure 23.)

As seen in Table IV the VRM axes  $1\sigma$  repeatability was  $4.3$ ,  $2.5$  and  $3.5 \mu\text{g}$  compared to  $13$ ,  $17$  and  $3.3 \mu\text{g}$  for the respective instrument axes. All results are considered satisfactory.

2.9  $\mu\text{g}$  ( $1\sigma$ )



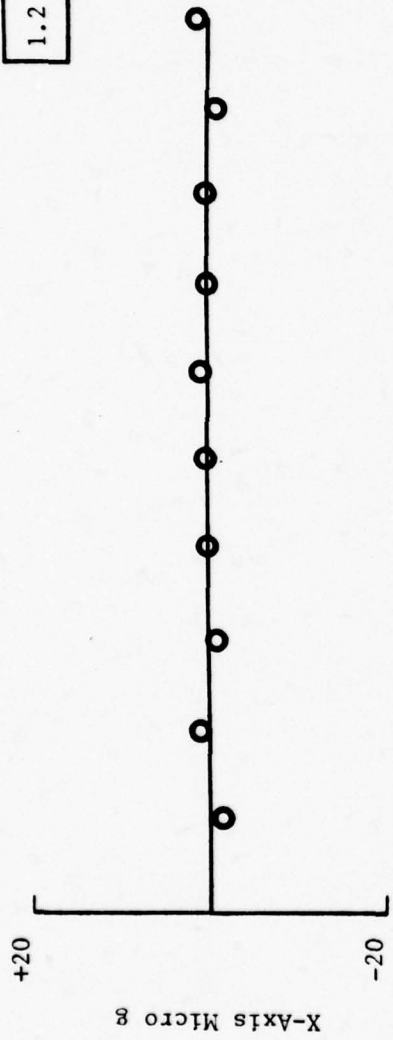
2.45  $\mu\text{g}$  ( $1\sigma$ )



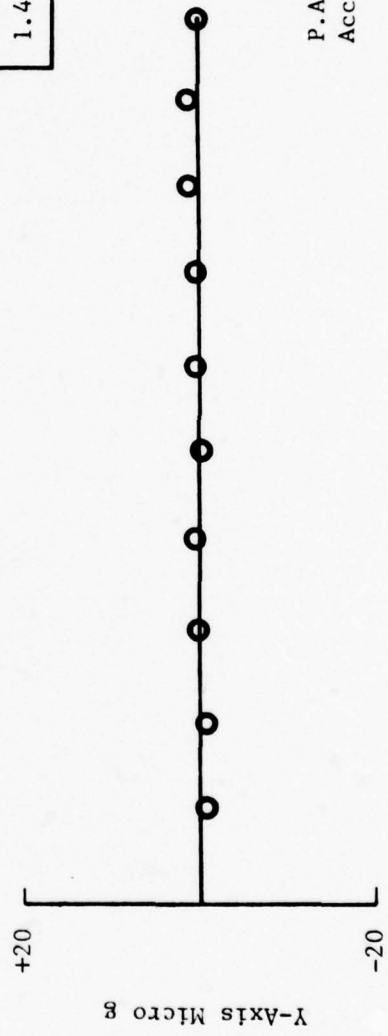
P.A. Horizontal  
X<sub>T</sub> Down  
Accelerometer #10

Figure 13. Short Term Repeatability

1.2  $\mu\text{g}$  / (10)



1.4  $\mu\text{g}$  (10)



P.A. Up  
Accelerometer #10

Figure 14. Short Term Repeatability

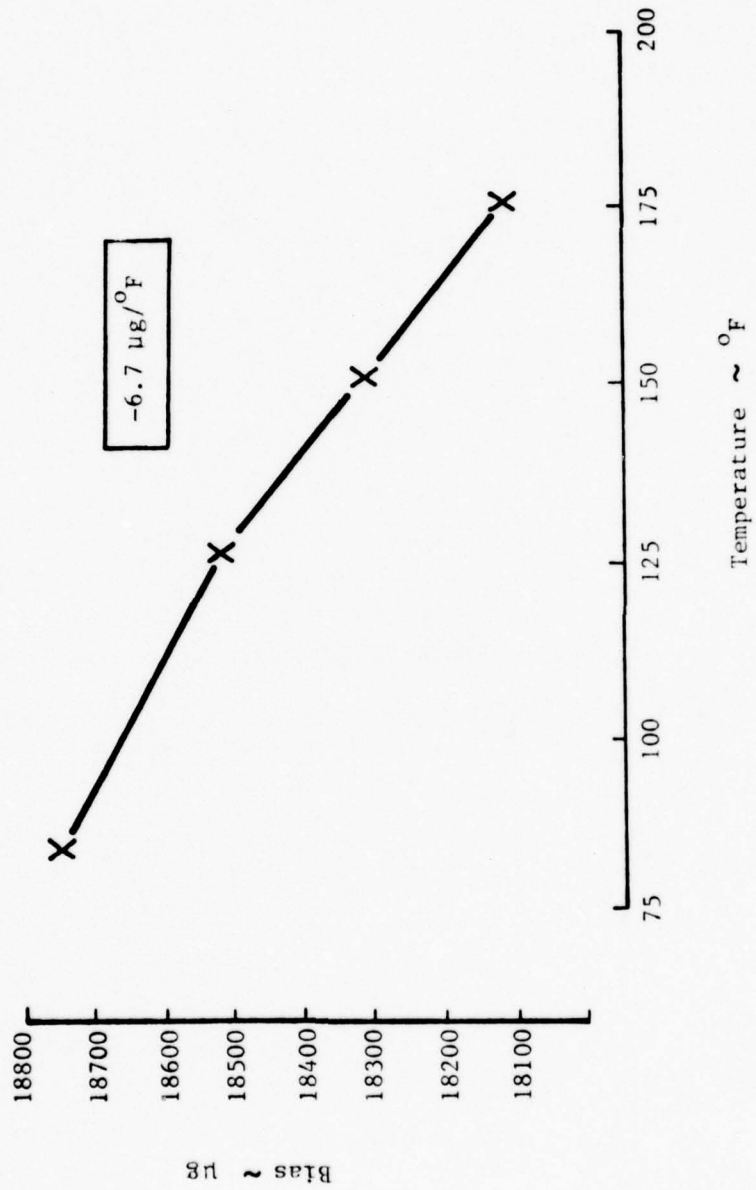


Figure 15. Uncompensated Bias Temperature Sensitivity - S/N 7S

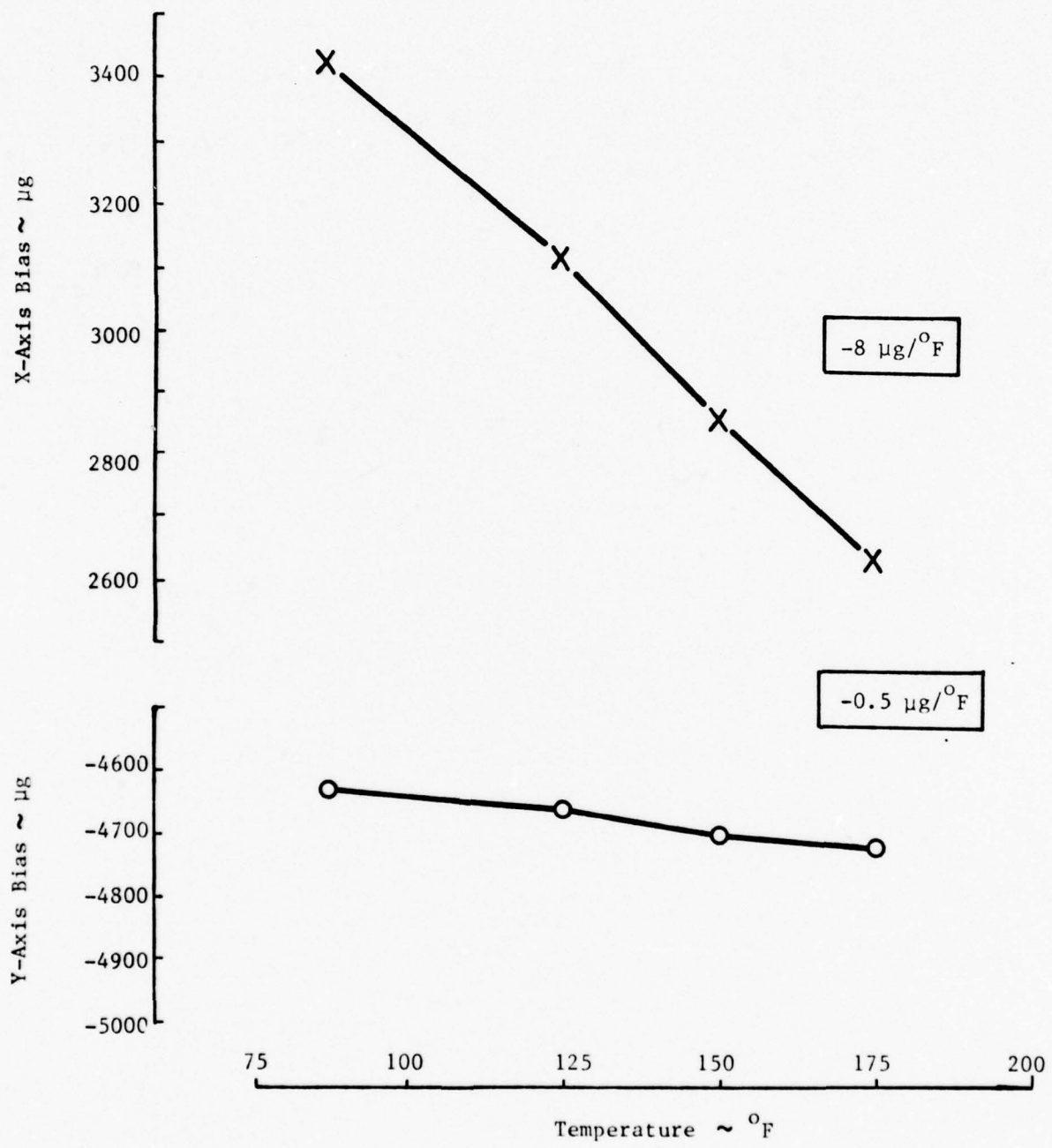


Figure 16. Uncompensated Bias Temperature Sensitivity - S/N 8

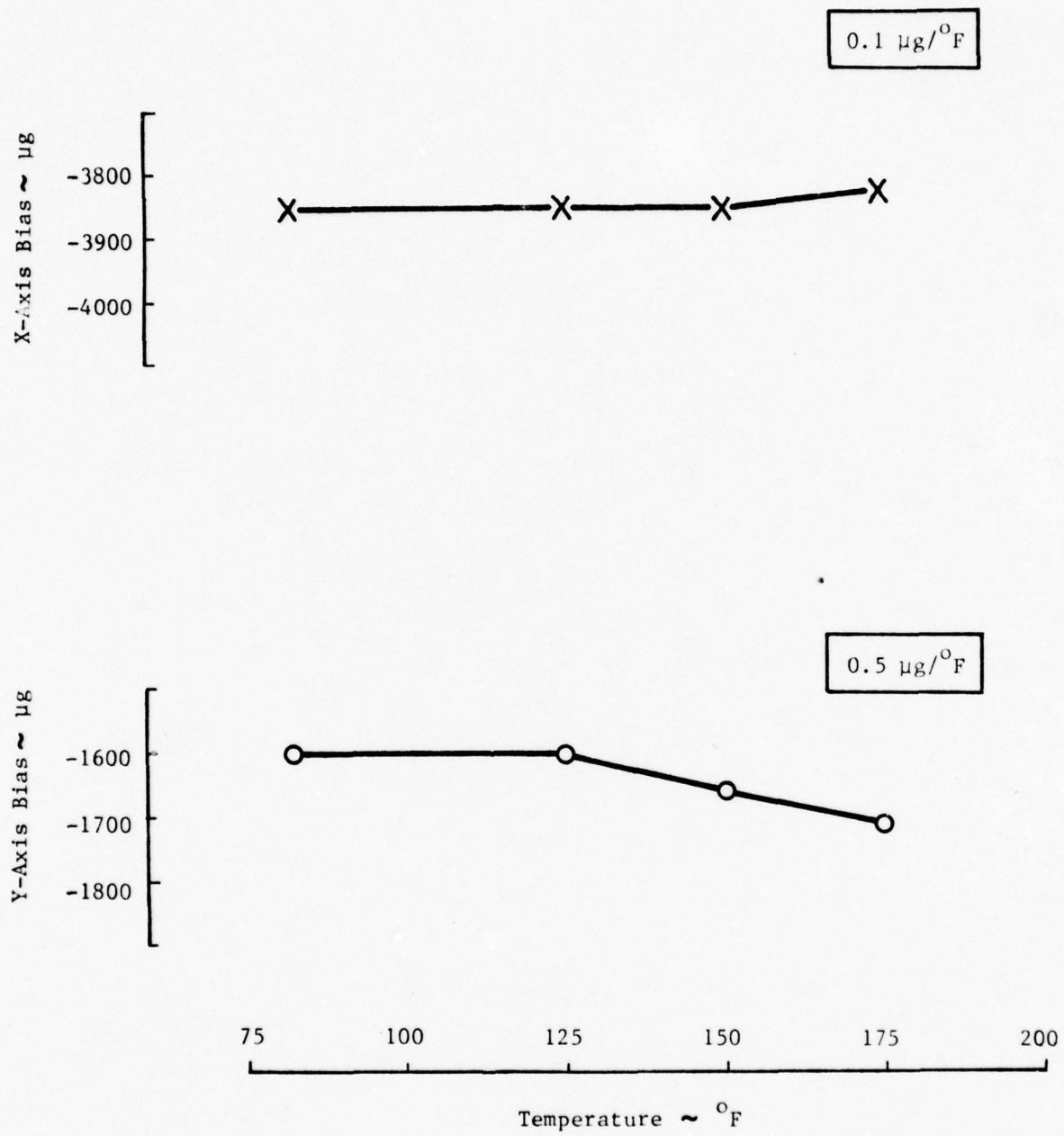


Figure 17. Uncompensated Bias Temperature Sensitivity - S/N 9

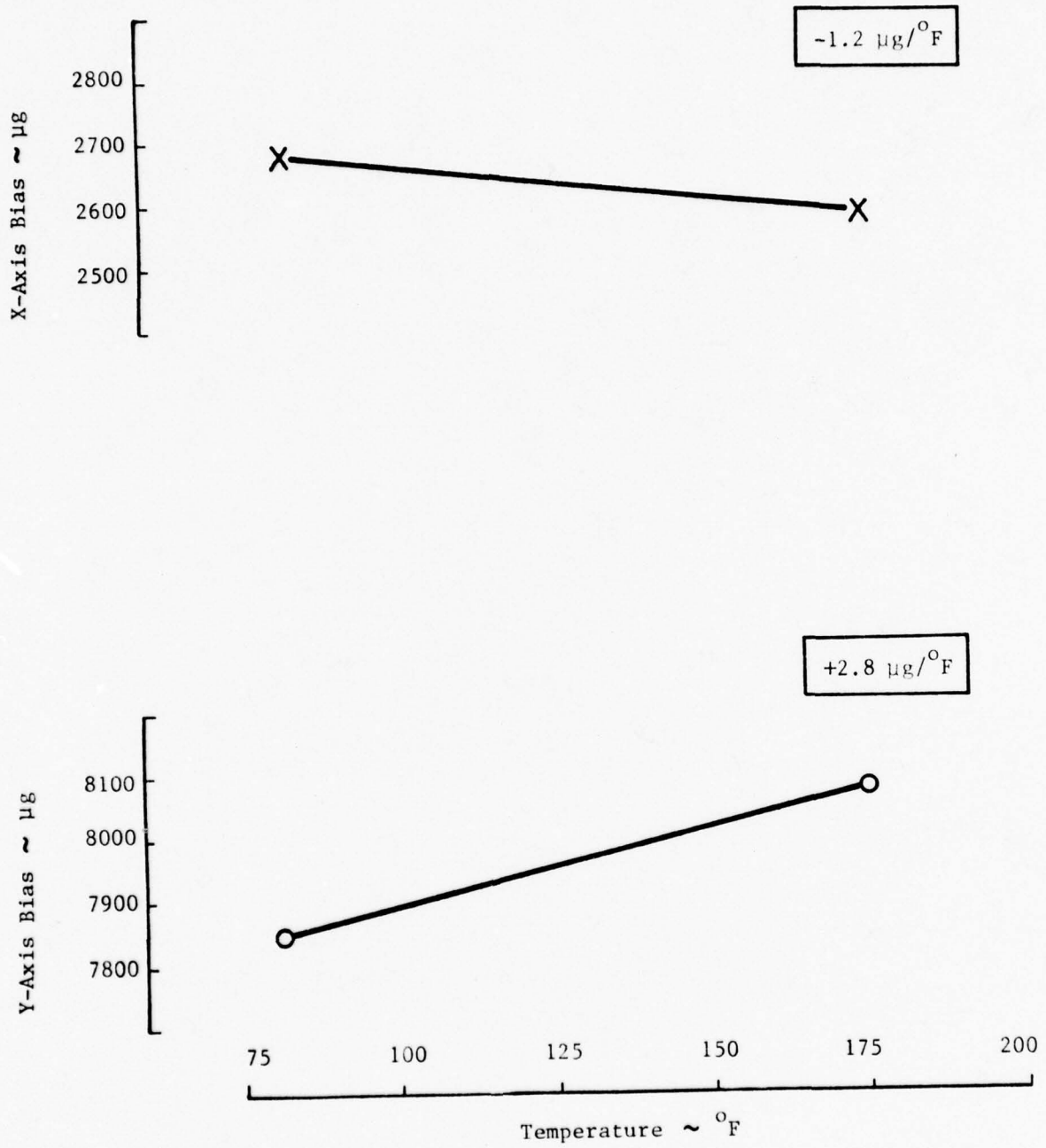


Figure 18. Uncompensated Bias Temperature Sensitivity - S/N 10

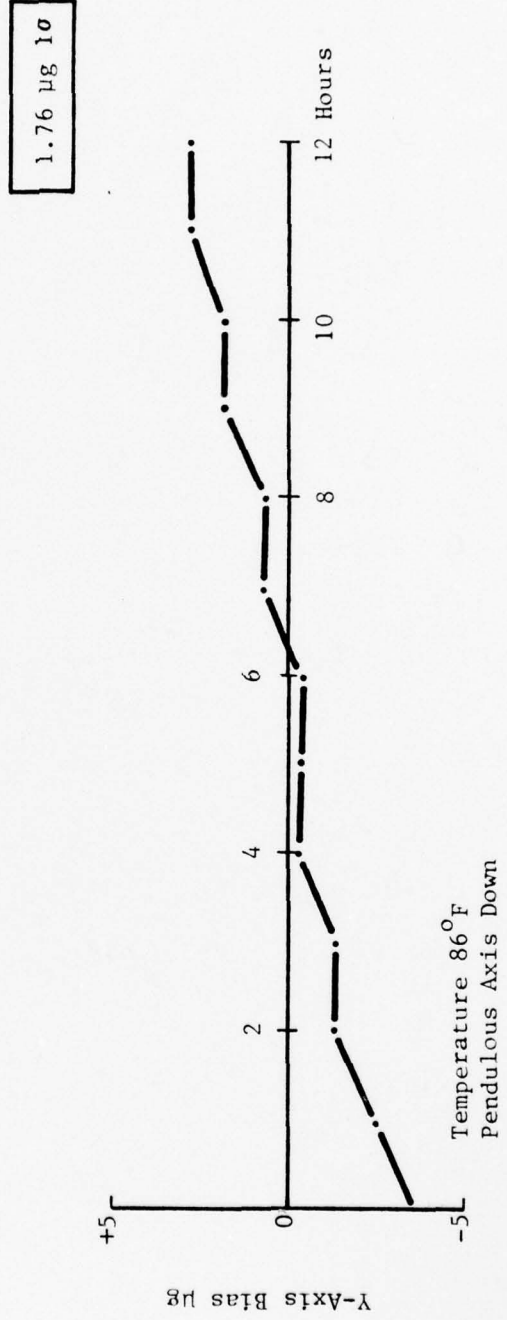
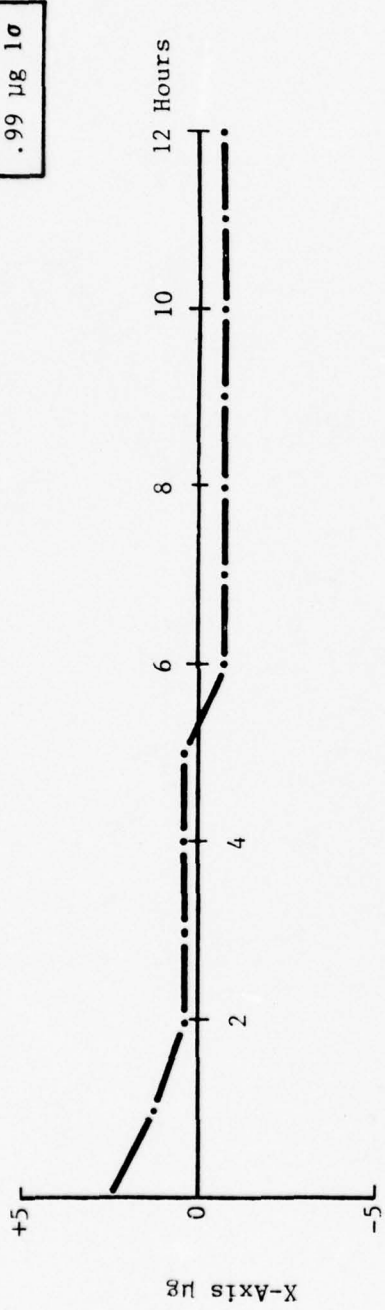


Figure 19. Bias Drift Accelerometer S/N 8

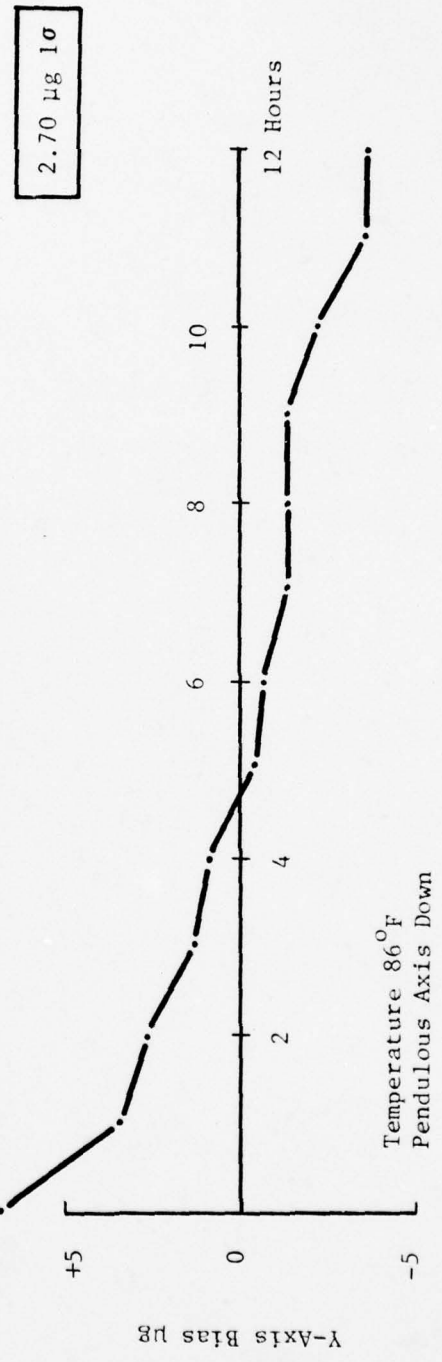
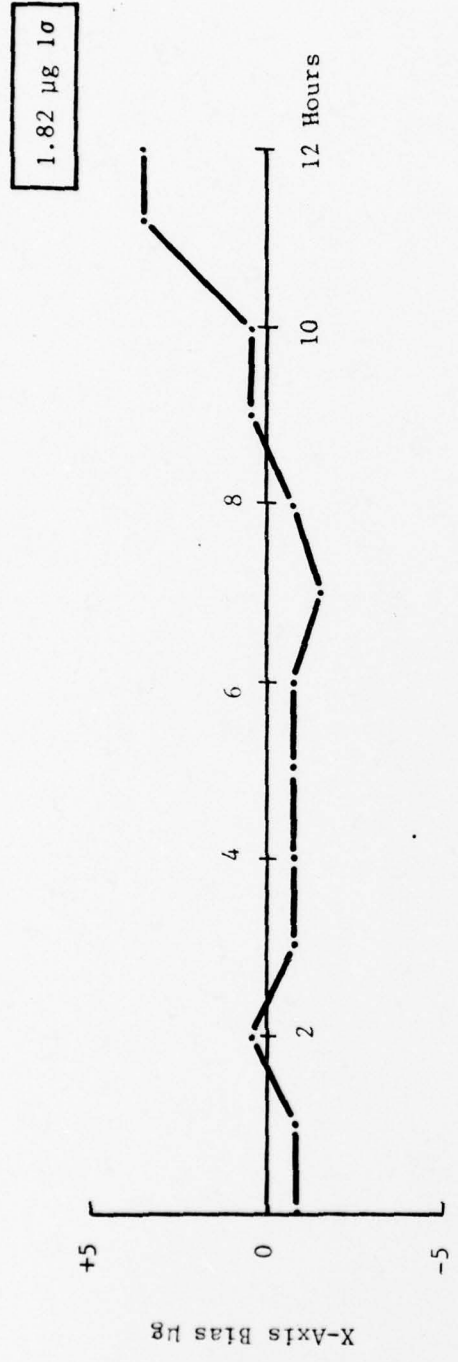


Figure 20. Bias Drift Accelerometer S/N 9

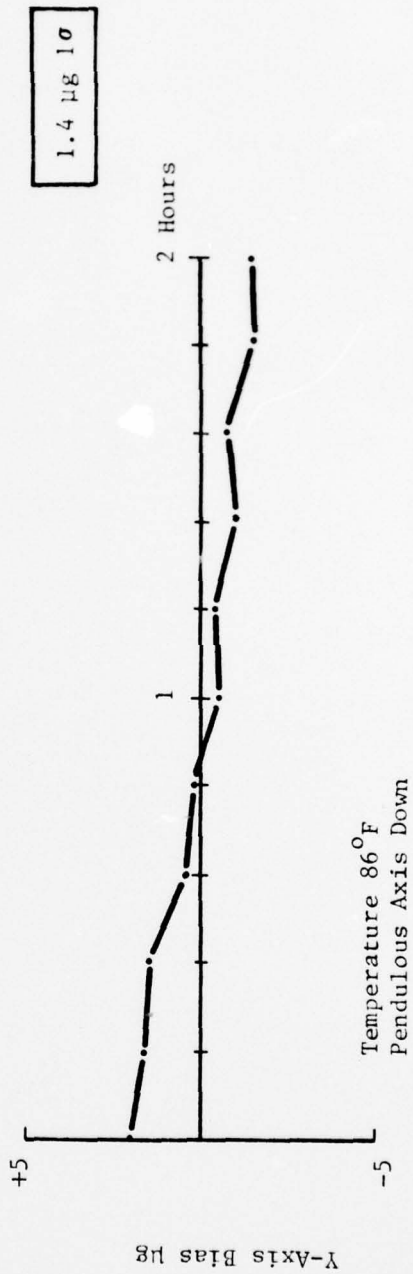
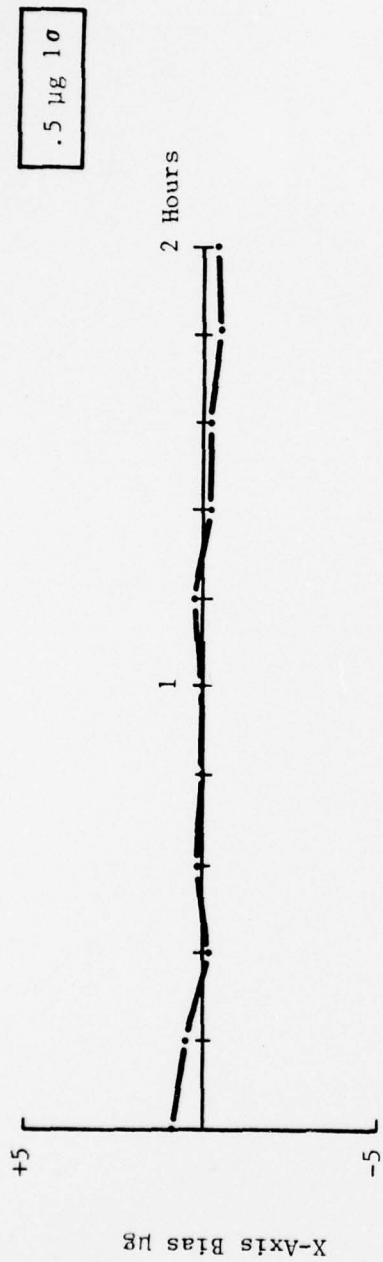


Figure 21. Bias Drift Accelerometer S/N 10

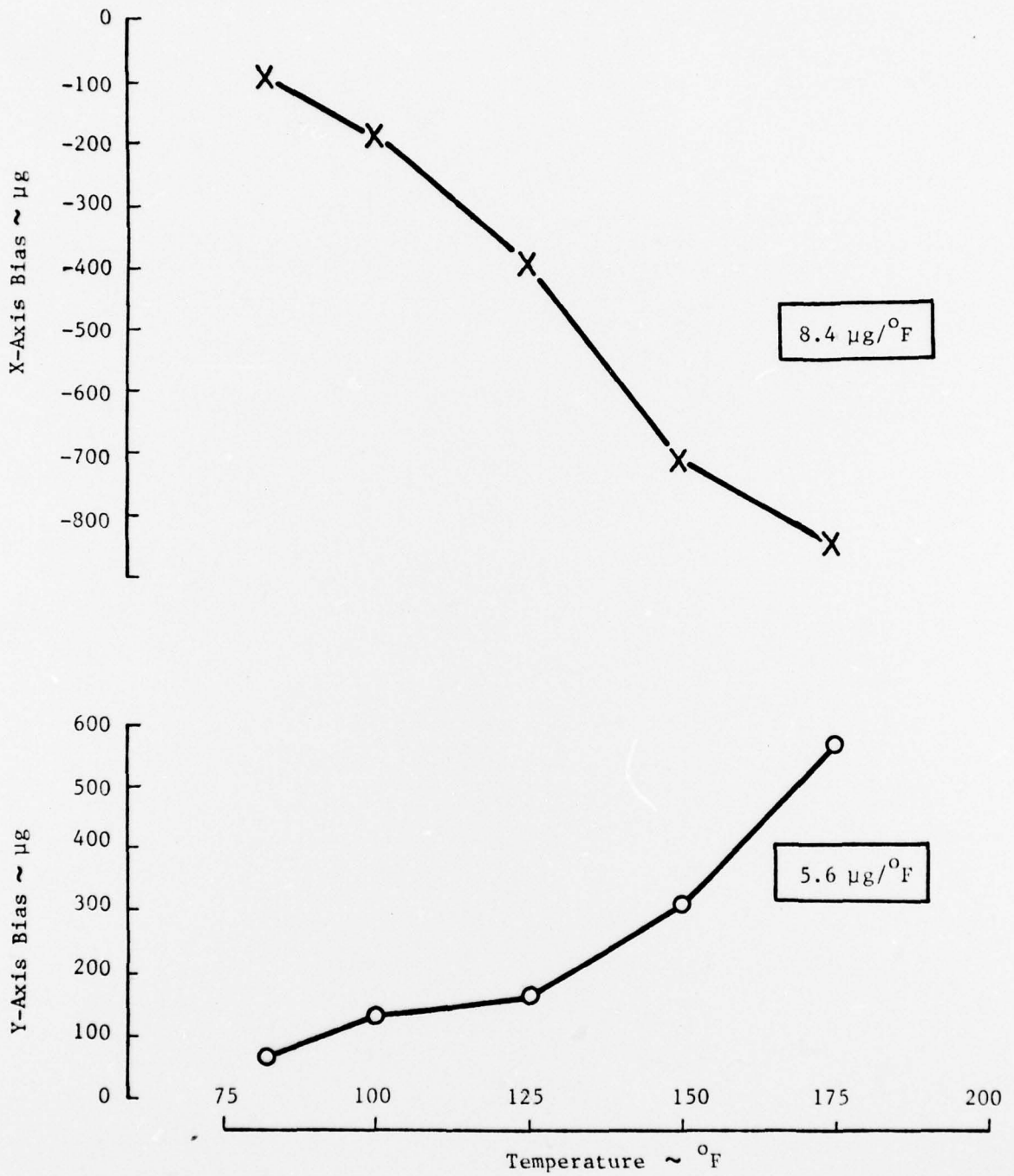


Figure 22. Bias Temperature Sensitivity - S/N 8 in VRM

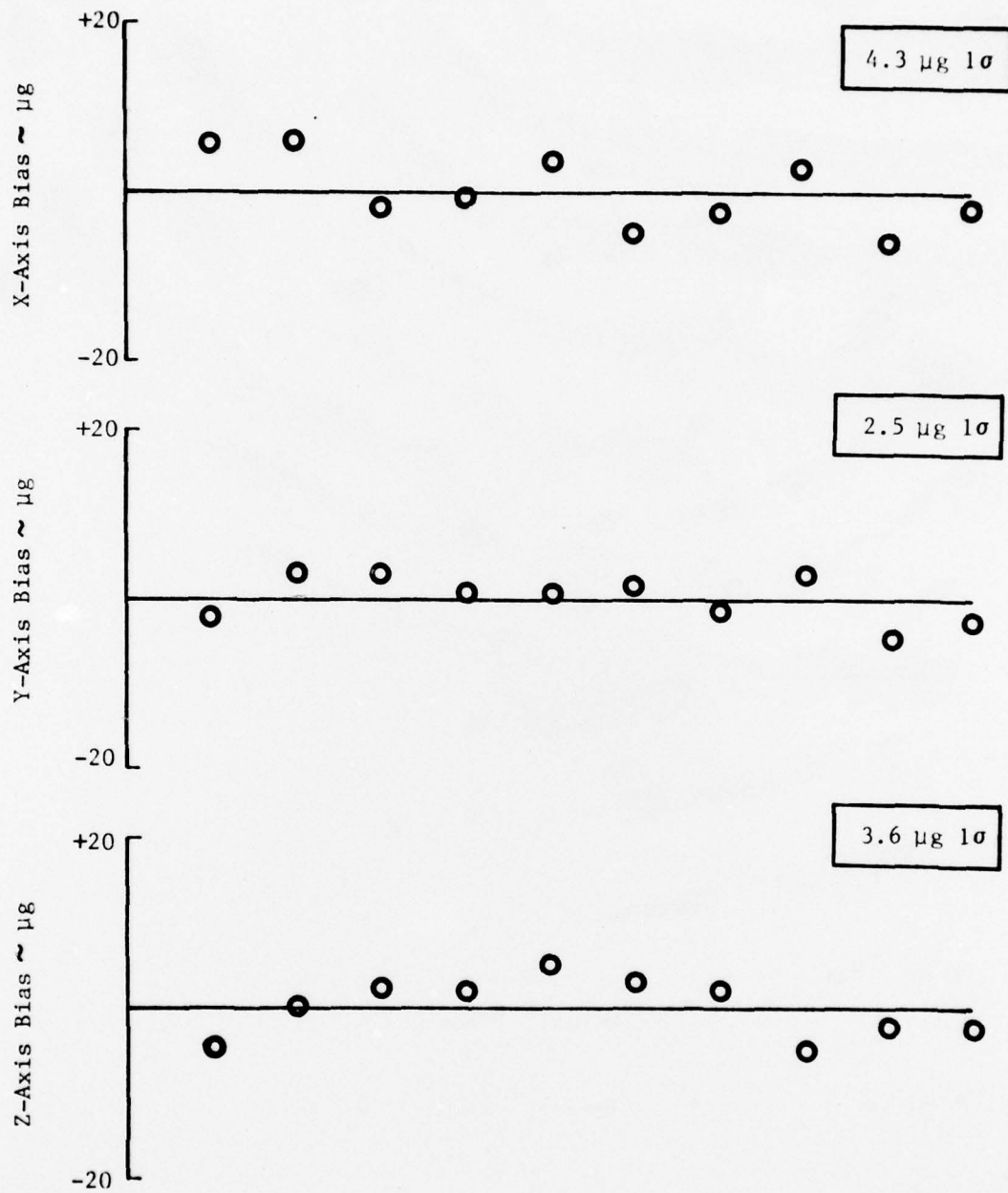


Figure 23. VRM Short Term Bias Repeatability

TABLE IV. SUMMARY OF VRM PERFORMANCE

Parameter	Units	Goal (Spec) (1)	Measured Axis		
			X	Y	Z
Bias Temperature Sensitivity	$\mu\text{g}/^{\circ}\text{F}$	40	8.4	5.6	N.M.
Short Term Bias Repeatability	$\mu\text{g}$ ( $1\sigma$ )	15	4.3	2.5	3.6
Scale Factor Temperature Sensitivity	PPM/ $^{\circ}\text{F}$	<250	N.M.	N.M.	245
Scale Factor	v/g	.51	.8466	.8349	1.6068
Bandwidth	Hz	250	255	280	250
Input Range	g	10	$\pm 5$	$\pm 5$	$\pm 6.7$
P.O. Excitation Frequency Sensitivity	$\mu\text{g}/\text{Hz}$	N.R.	.148	.234	N.M.
Power Supply Voltage Sensitivity					
Bias	$\mu\text{g}/\text{v}$	100	<1	15	15
Scale Factor	PPM/v	100	$\approx 0$	11	26

(1) Specification values taken from document SP237054 Code Ident 51993, Charles Stark Draper Laboratory, Inc.

The scale factors were measured and not adjusted at this time. Adjustment is readily done by selecting precision resistors trimmed for each axis so that the restoring current per g equals the desired voltage per g. See Table V. The scaling resistor used is 40 ohms and  $\pm 12$  VDC is available from the caging amplifier power stage. The input range then is  $\pm 5$  "g" (see Table VI).

TABLE V. VRM TORQUER SCALE FACTOR

X	Y	Z
1.181230 g/v	1.197720 g/v	1.606820 g/v

TABLE VI. VRM INPUT RANGE

X	Y	Z
$\pm 5$ g	$\pm 5$ g	$\pm 6.7$ g

The VRM Z axis scale factor temperature sensitivity was measured with results exactly predictable. The scale factor changes proportional to the Samarium Cobalt magnetic flux. The thermal property of  $\text{SmCO}_5$  is known to be 240 PPM; the VRM Z axis is 248 PPM. See Figure 24.

The frequency response was measured on each caging loop. Table VII lists the results; all axes had greater than 250 Hz bandpass.

TABLE VII. VRM CAGING LOOP BANDPASS

X	Y	Z
255	280	250

Figure 25 shows the bias sensitivity versus pickoff excitation frequency. The nominal 48 kHz was varied over a wide range and the output of accelerometer No. 8 was measured. The X output changed  $.148 \mu\text{g}$  per Hz and the Y output changed  $.234 \mu\text{g}$  per Hz around the operating frequency.

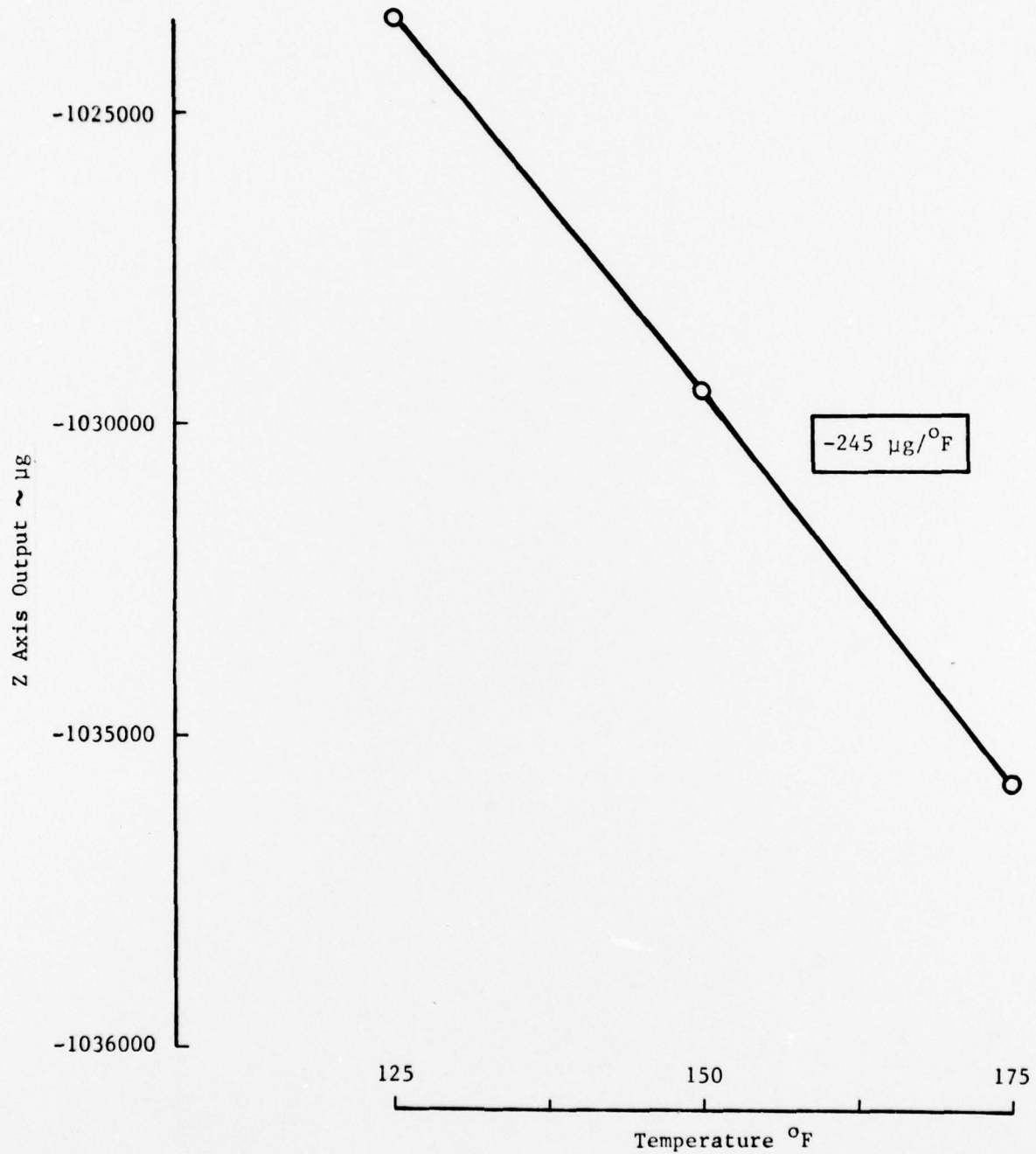


Figure 24. VRM Scale Factor Temperature Sensitivity

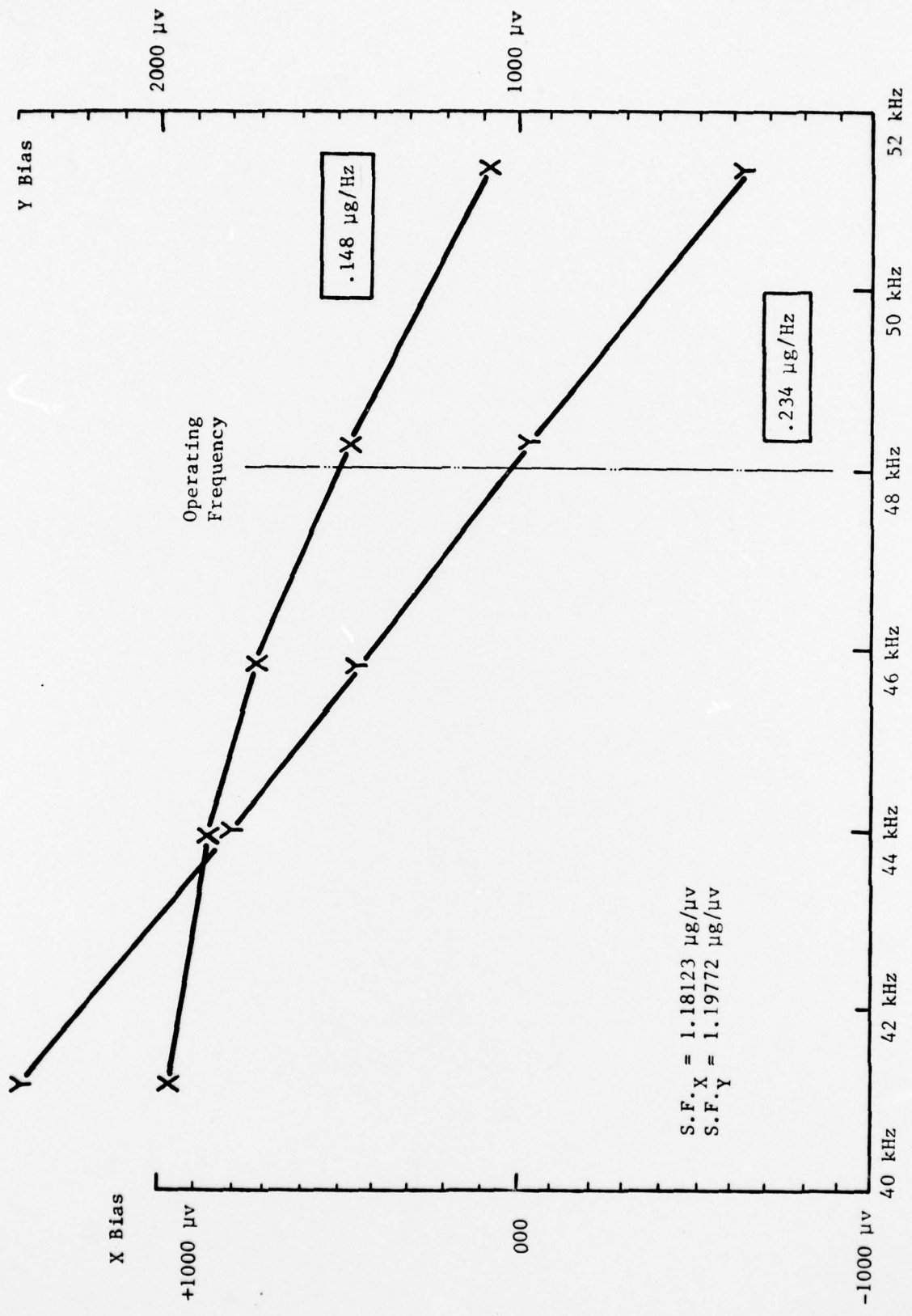


Figure 25. Bias Vs Pickoff Excitation Frequency

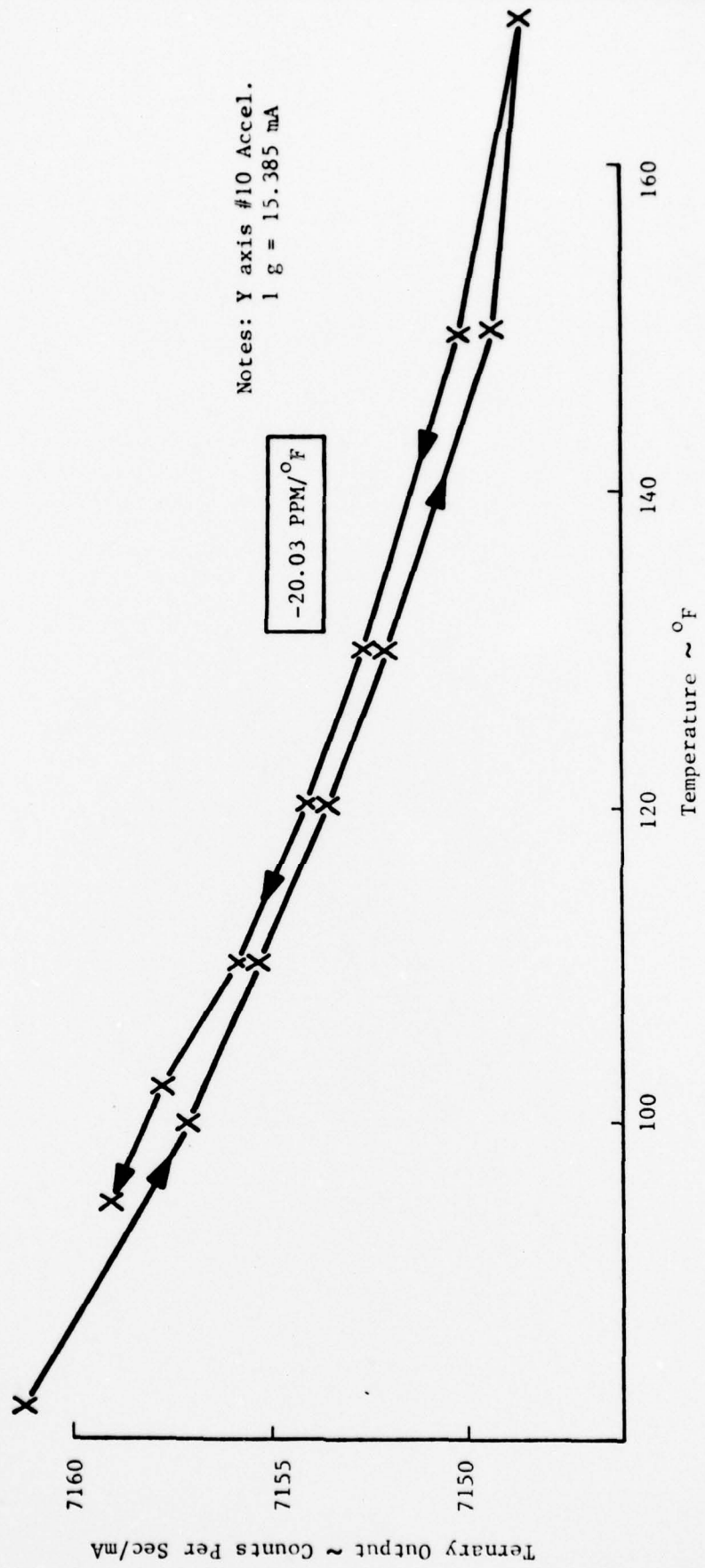
The  $\pm 15$  volt power to the VRM was changed between  $\pm 13.5$  VDC and  $\pm 16$  VDC. The bias and scale factor were measured at each voltage and is shown in Table VIII. Both changed significantly less than the specified  $100 \mu\text{g}$  per VDC and  $100$  PPM per VDC.

TABLE VIII. POWER SUPPLY VOLTAGE SENSITIVITY

Axis	Bias	Scale Factor
X	$0.87 \mu\text{g}/\text{v}$	$0.0 \text{ PPM}/\text{v}$
Y	$15.5 \mu\text{g}/\text{v}$	$11.4 \text{ PPM}/\text{v}$
Z	$15.3 \mu\text{g}/\text{v}$	$25.5 \text{ PPM}/\text{v}$
<p>① <math>+15</math> VDC and <math>-15</math> VDC changed <math>\pm 1.5</math> VDC simultaneously</p> <p>② Temperature <math>86^\circ\text{F}</math>.</p>		

The circuit boards were then subtested without the accelerometer to establish the temperature sensitivity of bias and scaling. Between room temperature and  $+170^\circ\text{F}$  the bias shift was immeasurable; less than one count per second which corresponds to  $9 \mu\text{g}$ . The scaling temperature sensitivity is  $-20 \text{ PPM}/^\circ\text{F}$  as shown in Figure 26. This is less than a tenth of the accelerometer temperature sensitivity due to the physical properties of Samarium Cobalt.

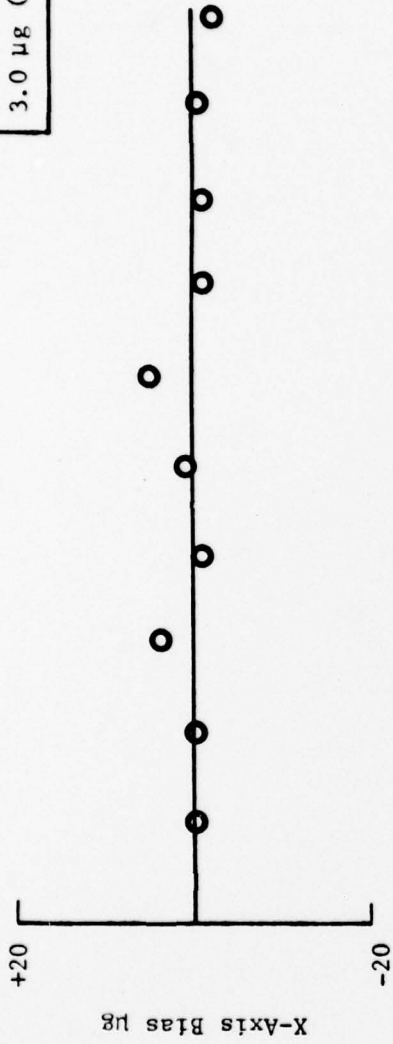
The closed loop repeatability with both analog and ternary digital caging is shown in Figures 27 and 28. All tests resulted in less than  $8 \mu\text{g}$  ( $1\sigma$ ) on each axis.



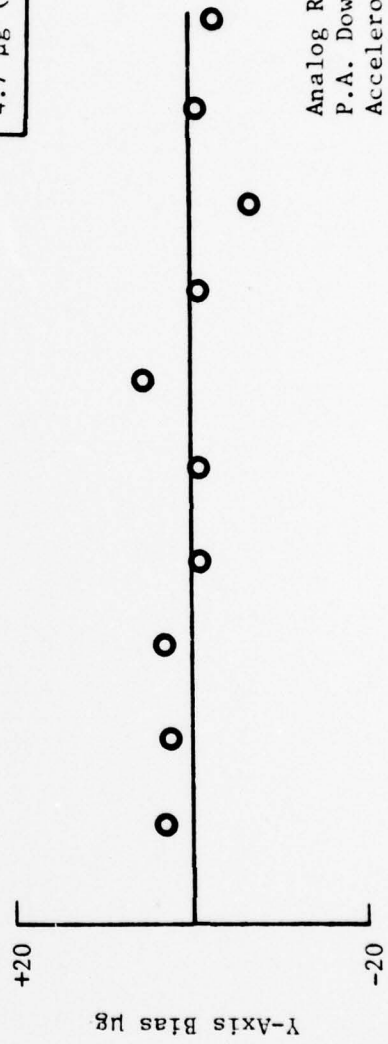
62-1A

Figure 26. Analog Conversion-Ternary Output Vs Temperature

3.0  $\mu\text{g}$  ( $1\sigma$ )



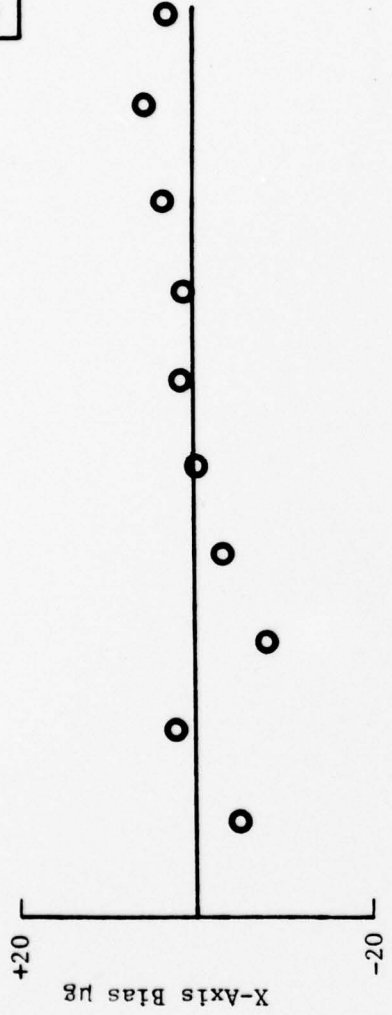
4.7  $\mu\text{g}$  ( $1\sigma$ )



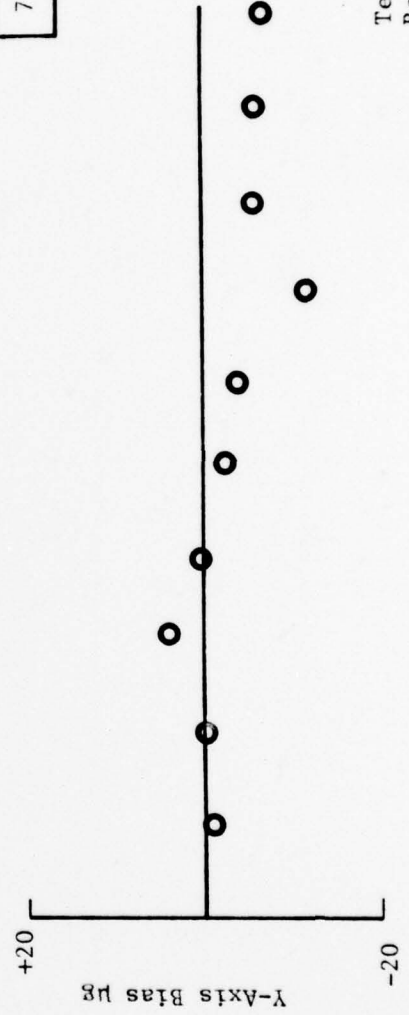
Analog Readout  
P.A. Down  
Accelerometer #10

Figure 27. Short Term Repeatability S/N 10

5.8  $\mu\text{g}$  ( $1\sigma$ )



7.6  $\mu\text{g}$  ( $1\sigma$ )



Ternary Digital  
Readout P.A. Down  
Accelerometer #10

Figure 28. Short Term Repeatability with Digital Output S/N 10

## VII. CONCLUSIONS

The overall accuracy demonstrated by the first two accelerometers of this design (built under the previous contract) illustrated that the design concept is sound. Of significance was the fact that performance could be accurately predicted prior to an accelerometer being built or tested. This demonstrated that the cause and effect of the component parts on performance can be analyzed, and design modifications made and various configurations established without large expenditures. Utilizing this fact, it was decided under this contract to modify the design to improve the long term bias stability. The design modification proved successful, and the performance, including exposure to many temperature cycles of  $-65^{\circ}\text{F}$  to  $+210^{\circ}\text{F}$ , was acceptable.

Some improvement has been made in the torquer efficiency. The size constraint and practicality of fabrication with small gaps put limits on the extent of improvement that was possible within the scope of work attempted. However, some change in the design is still possible to further improve the torquer efficiency.

Analysis of the scale factor temperature coefficient indicated the preferable way to lower this term is with electronic (or computational) compensation. Consequently, a transistor type temperature sensor in a TO-18 package was incorporated into the design. This sensor has a linear current change as a function of temperature output. The current can be scaled to give a relatively large voltage change as a function of temperature.

The work done to provide a digital output from the accelerometer showed that the accelerometer can be digitally torqued with a binary or ternary input. It also showed that analog torquing could be digitized to provide enough accuracy without temperature control for accurate navigation requirements. Due to considerations of bandwidth and bias temperature sensitivity, analog torquing with a current-to-digital conversion was considered the best of the methods tried.

## VIII. RECOMMENDATIONS

- (1) The design change to improve the bias stability proved successful, but the design at present utilizes an epoxy joint between the suspension and pendulous mass. This makes it impossible to remove the pendulous mass for in-process assembly or repair. There is space available in the design to make a threaded connection between these parts, and it is recommended that the design be modified to accomplish this.
- (2) The suspension geometry and flexure thickness have not been optimized for performance, especially relative to vibration and shock inputs. Consideration should be given to modifying the suspension to give the best results for environmental inputs.
- (3) The torquer current as a function of acceleration is still higher than desirable. Work should be continued to reduce this.